Establishing a Model to Label and Stimulate Cells Active During Motor Behaviour

Marc Vani

Thesis submitted to the Faculty of Graduate and Postdoctoral Studies in partial fulfillment of the requirements for the Master of Science degree in Neuroscience

Department of Cellular and Molecular Medicine

Faculty of Medicine

University of Ottawa

Abstract

The remapping of cortical networks after stroke is hypothesized to be one of the mechanisms subserving functional recovery. Our understanding of cortical remapping remains limited due to the inability to resolve which cells are active while performing motor tasks with high temporal and spatial specificity.

The experiments presented in the first chapter of this thesis evaluate the ability of the inducible Arc-CreER^{T2}:Rosa-YFP$^{f/f}$ model to label cells in the motor cortex activated by a motor-related behaviour. Through the modification of previously published 4-hydroxytamoxifen treatment paradigms, this model can differentiate between animals that performed the rotarod task at two time points and home cage controls. In addition, 65% of cells active at the first behavioural time point are reactivated. Taken together, these data suggest that the Arc-CreER^{T2}:Rosa-YFP$^{f/f}$ model is able to reliably label networks used to perform the same behavioural task at two time points.

The second chapter of this thesis details a pilot study in which the Arc-CreER^{T2}:Rosa-ChR2:YFP$^{f/f}$ model was used to test the effect of daily optogenetic stimulation of the contralateral cortex on functional recovery. The results of this chapter suggest that stimulating the contralesional motor cortex may impair functional recovery. Overall, the results of this thesis lay the foundation to use this model to investigate motor networks in both naïve and pathological conditions, such as stroke.

TABLE OF CONTENTS

List of Figures

List of Abbreviations

CA3	Cornu Ammonis region 3
ChABC	Chondroitinase ABC
ChR2	Channelrhodopsin-2
CreER	Cre-estrogen receptor recombinase
CSPG	Chondroitin sulfate proteoglycans
DAPI	diamidino-2-phenylindole
DG	Dentate gyrus
DMSO	dimethyl sulfoxide
EtOH	Ethanol
FF	free-floating
GECI	Genetically encoded calcium indicator
GFP	Green fluorescent protein
IEG	Immediate early gene
IHC	Immunohistochemistry
LCN	Lateral cerebellar nucleus
M1	Primary motor cortex
M2	Secondary motor cortex
MAG	Myelin-associated glycoprotein
MCAo	Middle cerebral artery occlusion
NaN_3	Sodium azide
OH-Tam	4-hydroxytamoxifen
PBS	phosphate-buffered saline
PFA	paraformaldehyde
PNN	Perineuronal net
SSRI	Selective serotonin reuptake inhibitor
tDCS	Transcranial direct current stimulation
rTMS	Repetitive transcranial magnetic stimulation
SBR	Spontaneous biological recovery
TRAP	Targeted recombination in active populations
Tween-20	polyoxyethylenesorbitan monolaurate
VNS	Vagal nerve stimulation
YFP	Yellow fluorescent protein

Acknowledgements

First and foremost, I would like to thank my family, who have been a constant source of support, encouragement, and wisdom.

I would also like to thank my labmates, collaborators, and the Canadian Partnership for Stroke Recovery, without whom this project would have never come to fruition.

Finally, I would like to thank my supervisor, Diane, who took me into her lab as a second-year undergraduate student and provided me with a constant stream of opportunities to grow as both a scientist and a person. Thank you for being such an exceptional mentor and teacher.

1. Introduction

This thesis describes the establishment of a mouse model to label cells in the motor cortex recruited during a behavioural task, and a pilot study using optogenetics to probe the effect of contralesional cortex stimulation on stroke recovery. Within this introduction, essential background on stroke recovery and models to investigate cortical reorganization is described.

Stroke

A stroke occurs when all or part of the brain stops receiving blood resulting in cell death[1]. Strokes are classified as either haemorrhagic or ischemic depending on how the affected area is deprived of blood, and can be further categorized based on the number or size of vessels affected, as well as the location of the infarct. Haemorrhagic strokes are caused by a rupture of one or many blood vessels in the brain, which causes uncontrolled bleeding. Haemorrhagic strokes are often fatal, and fortunately only account for approximately 10% of all strokes[2]. The remaining 90% of strokes are ischemic, which occur when part of the brain is deprived of blood due to the presence of a clot in an artery or arteriole[1]. The blockage deprives the area of blood and nutrients, disrupting cellular processes such as oxidative phosphorylation, which leads to an interruption in adenosine triphosphate production, and the initiation of a cascade of cellular processes ultimately leading to cell death[3].

Approximately 40,000 Canadians suffered a stroke in 2017[1]. Almost 80% of these people survived their stroke, and most joined the over 400,000 survivors living with disabilities caused by stroke[1]. Over 40% of stroke survivors suffer from moderate to severe disability[1]. Further, the number of patients living with the effects of stroke is expected to

double in the next 20 years[1]. Not only is there an increase in emotional and physical support required for stroke survivors, but there is also a large financial burden suffered[4]. Stroke leads all other neurological conditions in Canada in terms of direct costs. It is estimated to cost Canadians $2.5 billion per year[4].

Collaborative efforts among institutions to author guidelines on stroke care have increased the number of stroke survivors and has improved the care stroke survivors receive. Most notably, the development of *The Canadian Stroke Best Practice Recommendations* document was penned to offer information on the continuum of care required for stroke patients[5]. These guidelines touch on a multitude of topics, from the importance of knowing the three signs of stroke (facial drooping, weakness in one or both arms, and slurred speech), allowing more patients to receive acute care, to providing recommendations regarding physical rehabilitation.

Approved treatments for stroke

The incidence of stroke is on the rise, however there is also a larger percentage of patients surviving than ever before. This is partially due to important advances in acute care, such as the development of thrombolytic agents. Tissue plasminogen activator (tPA), approved in 1996, is the only approved drug to treat acute stroke[6]. When administered intravenously, tPA acts to dissolve clots, thus restoring blood flow to an occluded area of the brain[6,7]. Another successful acute treatment for stroke patients has been endovascular surgery. This technique, famously shown to be effective at treating stroke in the double-blind ESCAPE Clinical Trial (ESCAPE: Canadian Endovascular treatment for Small Core and Anterior circulation Proximal occlusion with Emphasis on minimizing computerized axial tomography to recanalization times)[8]. This surgical treatment involved inserting a thin tube into an artery in the patient's leg and guiding it towards the clot in the brain. Once

the tube arrives at the clot, a stent is used to remove the clot[8-10]. While both tPA and endovascular surgery have been shown to be effective, both must be administered in a relatively short window (five and seven hours after stroke onset, respectively)[9]. Nevertheless, they have been effective in acute cases in restoring blood flow to the affected areas and thus reducing, and in some cases reversing the effects of stroke, thus reducing the number of deaths from stroke.

For those afflicted with stroke-induced disability, rehabilitation is viewed as the gold standard of care for achieving maximal long-term recovery, and because of the wide range of deficits experienced by stroke patients, rehabilitation is often administered in a multidisciplinary way[11]. Strategies such as the inclusion of exercise and fitness components are common. Constraint-induced movement therapy (CIMT) can also be used as a method of restricting the use of the non-paretic limb and is often used in concert with rehabilitation to encourage usage of the affected limb[11]. Although rehabilitation has been shown to be effective[12,13], only 37% of patients with moderate to severe deficits receive access to standard rehabilitation[14]. Furthermore, patients who do not make use of these treatments often only achieve a partial recovery[15]. These factors illustrate the urgency with which new treatments must be developed.

Preclinical studies and clinical trials in stroke recovery

Remarkably, in the absence of treatment both patients and pre-clinical models of stroke demonstrate a limited degree of recovery. This recovery, termed spontaneous biological recovery (SBR) is thought to be due to many different processes. For example, the resolution of a brief period of diaschisis and edema and reduction in inflammatory molecules are thought to partially underlie the early phases of SBR[16]. Later during SBR, a growing body of literature suggests a contribution of multiple processes, such as

angiogenesis, neurogenesis, and reorganization of functional circuits[15]. Many experimental treatments and interventions for stroke patients seek to enhance recovery by targeting these mechanisms. Tested interventions include chemical and biological treatments, as well as novel rehabilitation techniques.

The importance of growth factors during development led researchers to believe that they could be important for repair after stroke. Preclinical studies supported this idea, with molecules such as brain-derived neurotrophic factor[17] and erythropoietin[18] administration significantly improving behavioural outcomes in animal models of stroke. Less success has been observed in human patients treated with growth factors. This is perhaps due to the difficulty that large molecules such as growth factors have in crossing the blood-brain barrier (BBB), which therefore limits their ability to reach the site of injury[19]. This difficulty crossing the BBB is shared by other large molecules, such as monoclonal antibodies. These molecules are designed to bind to and neutralize molecules that prevent growth, and thus facilitating recovery by creating an environment permissive to growth[20]. One such target is myelin-associated glycoprotein (MAG), which prevents axonal growth. In a trial in which the humanized anti-MAG antibody GSK249320 was administered 24-72 hours and then 9 days post-stroke, no significant improvements in gait velocity were observed[21]. However, the antibody was well-tolerated, and no safety concerns were identified. The authors hypothesized that the failure to detect a significant improvement in patients which received antibody treatment could be because the antibody did not reach the target. This suggests that advances in shuttling large molecules across the BBB need to be made before antibodies can become effective tools for stroke recovery.

Small molecules, such as selective serotonin reuptake inhibitors (SSRIs), have enjoyed much greater success, and have even been used in large-scale double-blind trials. Most notably, in the FLAME trial (FLAME: Fluoxetine for motor recovery after acute ischaemic stroke), patients given SSRIs after stroke had significantly better outcomes at 90 days post-stroke[22]. Not only did the mood of those treated with SSRIs improve significantly, but these patients also displayed an almost 10-point increase in Fugl-Meyer score at 90 days post-stroke, even after adjustments for treatment centre, age, and history of stroke. The authors hypothesized that this effect could be due to the serotonergic system providing facilitation to the motor system, which would make sense, since SSRI treatment was paired with rehabilitation training[23].

Preclinical studies have also suggested other promising targets for stroke recovery. One well-researched molecule is chondroitinase ABC (ChABC), which dissolves chondroitin sulfate proteoglycans (CSPGs). CSPGs are a component of perineuronal nets (PNNs), which act to restrict plasticity in the brain by surrounding the soma and proximal dendrites of neurons[24]. Thus, by partially dissolving PNNs around the stroke or along the corticospinal tract, the opportunity for plasticity is enhanced, which could lead to enhanced recovery. A recent meta-analysis of studies using ChABC in pre-clinical studies of stroke suggests that this treatment is effective in improving behavioural outcomes in animal models of stroke[25]. The hope of translating this treatment to human patients is promising, especially when considering recent advances in controlling the expression of ChABC[26]. However, many experimental treatments like ChABC have yet to face the test of clinical trials.

Stimulation Therapies to Enhance Stroke Recovery

Studies of SBR, and specifically cortical reorganization, identified and described the reallocation of functions that were previously under the control of the afflicted region to other central nervous system regions. Some regions that have been shown to be implicated in this process are the peri-infarct regions[27], as well as other distinct cortical regions such as the non-affected contralateral hemisphere[28], the pre-motor cortex[29], and the spinal cord[30]. Additionally, in both humans and preclinical models of stroke, changes in excitatory-inhibitory balance of neural networks after ischemia are well-documented. Specifically, after stroke, the lesioned cortex is hypothesized to exert a reduced transcallosal inhibition of the contralesional hemisphere, while the contralesional hemisphere exhibits an increased transcallosal inhibition of the ipsilesional hemisphere[31]. This results in an increase in excitability of the contralesional cortex, and a suppression of the ipsilesional hemisphere. During the acute phase of recovery, intracortical disinhibition of both the lesioned and unlesioned hemispheres is associated with recovery[31], while the chronic phase of recovery is also associated with the organization of new circuits[32-34]. Importantly, these changes occurring during SBR happen during a "critical window" of plasticity in the weeks following a stroke[15,35-38].

Case studies and clinical trials using stimulation therapies for stroke recovery have largely focused on either reducing the deleterious overexcitability of the contralesional cortex or increasing the excitability of the ipsilesional cortex. Previous and current clinical trials have largely used either repetitive transcranial stimulation (rTMS) or transcranial direct current stimulation (tDCS). During rTMS, an electromagnet is placed above a brain area of interest. By passing a current through the electromagnet and creating a brief magnetic field, neural activity in the underlying neurons can be modulated. Low-frequency

rTMS involves stimulating the brain at <1 Hz, and causes local inhibition of the underlying neurons, while high-frequency rTMS involves stimulating at >3 Hz which activates the underlying neurons. A recently published summary regarding the clinical use of rTMS in stroke recovery included almost 1000 stroke survivors in placebo-controlled trials that are using either high- or low-frequency rTMS[39]. This review reported highly inconsistent findings regarding treatment efficacy[40,41].

TDCS involves placing electrodes on both sides of the head and passing a current through them to modulate cortical excitability[41,42]. Although little is known about the underlying neurophysiological mechanisms, tDCS has proven to not only be effective in certain cases, but also affordable, convenient, and simple to use. These aspects make it a particularly attractive option for stroke treatment in an era of healthcare spending cuts. Most importantly, a recent review found that for the treatment of motor deficits, tDCS was only useful when used in the chronic phase of stroke recovery, but not the acute and sub-acute phases[42].

Some researchers have sought to use other means of stimulation to enhance stroke recovery. For example, in a rat model of stroke, it has been shown that vagal nerve stimulation (VNS) paired with rehabilitation more than doubled rats' performance on an untrained reaching task compared to rehabilitation alone[43]. This effect is likely because VNS paired with forelimb movements increases the representation of the forelimb in the motor cortex, as has been shown in studies of the naïve rat brain[44]. In humans, it has been shown in a small pilot study of 20 patients that VNS is not only safe and well-tolerated in stroke patients[45]. Furthermore, when paired with rehabilitation, VNS results in a six-point

increase in Fugl-Meyer score over patients that received rehabilitation alone. Thus, this is a potentially promising avenue of approach to treat stroke patients.

Clinical trials making use of stimulation techniques have become numerous in the past years, and despite their increasing success, fundamental questions remain with respect to the biological mechanisms underlying these improvements[46-48]. Further, it is unknown what types of cells take up the function of the infarcted region, and when they are becoming active. Answering these questions will be crucial for the optimization of stimulation paradigms, as well as to inform when and what areas and cell types would be best to stimulate. In order to answer these questions, preclinical studies have begun using optogenetic approaches to either stimulate or silence specific population of cells during stroke recovery.

Pre-clinical stimulation and cortical reorganization studies

Pre-clinical studies of stroke have begun to shed light on which areas would be ideal targets for stimulation therapy at various times during recovery as well as the mechanisms underlying these effects. Of the many targets identified, the most intensively studied has been the peri-infarct. Steinberg group demonstrated in a study that stimulation of the ipsilesional primary motor cortex (M1) promoted functional recovery in a middle cerebral artery occlusion (MCAo) model of stroke[49]. This was done using a Thy-1-ChR2 mouse, which allowed for the expression of the light-activated cation channel channelrhodopsin-2 (ChR2) in excitatory layer V neurons. The authors hypothesized that these effects were likely due to the increased expression of various neurotrophic factors, which enhanced plasticity in the cortex after stroke. Using the same tools, the same group published another paper three years later demonstrating that stimulation of the lateral cerebellar nucleus (LCN) also improved stroke recovery[50]. The authors hypothesized that

because the LCN provides excitatory input to the cortex, stimulation of the LCN provided excitatory input to the ipsilesional cortex, allowing for an increase in expression of neurotrophic factors in this region. These studies clearly support the ongoing clinical work of stimulating the lesioned cortex.

The role of the contralesional cortex in stroke recovery has remained much more controversial. Until recently, decreasing contralesional M1 excitability was thought to improve recovery[51]. It would therefore follow that increasing the excitability of the contralesional hemisphere may reduce recovery. In disagreement with this hypothesis, Cheng et al. (2014) reported that contralesional M1 stimulation had no effect on recovery. This result is surprising, given that stimulation was done in a Thy1-ChR2 mouse, in which many neurons were stimulated. Other studies took the opposite approach for determining which areas are important for stroke recovery by selectively silencing specific areas of the brain. These studies found that contralesional inhibition can exacerbate or improve impairments based on the size of the stroke[52,53]. More specifically, they found that the inhibition of the contralesional hemisphere via lidocaine injections impairs motor performance with the stroke-affected paw, while others have shown its inhibition with muscimol improves motor recovery 4 weeks after stroke.

The lack of consensus on the efficacy of stimulation treatments and the role that various areas of the brain play in stroke recovery supports the call for more research into how motor networks reorganize after stroke. Therefore, to design well-informed clinical stimulation trials, it is necessary to determine not only the motor networks that arise to take up the function of the infarcted region, but also determine how these networks change.

Using immediate early genes (IEGs) to investigate the reorganization of functional circuits

Immediate early genes (IEGs) get their name from their activation kinetics. In response to neural activity, they are transcribed in a matter of a few minutes, and protein concentrations reach their peak within one to three hours, degrading soon afterwards[54,55]. Common examples of IEGs include c-Fos, Arc/Arg 3.1, zif268, and NPAS4.

These genes are often used as a marker of neural activity due to the quick and transient nature of their activation. In general, experiments making use of IEGs involve animals performing a behavioural task and sacrificing them at the time of peak protein concentration. After tissue processing, post-hoc immunohistochemistry (IHC) is done to visualize which areas express IEGs. With the proper controls, these types of experiments allow for conclusions to be drawn regarding the activity of a brain region during the behavioural task based on the presence or absence of IEGs. This technique is useful since all active neurons in the brain can be observed. Additionally, more precise determinations such as the location of the active neuron and colocalization analysis can be performed to determine the phenotype of the active neurons. This methodology has been used in stroke research and has been used to show that rats exposed to a combination of enriched rehabilitation and daily reach training had higher levels of IEG expression in the perilesional motor cortex and striatum, as well as contralesional motor cortex than rats that received either individual intervention, and standard housing controls[56].

A limitation of using IHC to examine IEG expression is that it cannot distinguish the degree of activation of each individual neuron. This is because the relationship between the signal achieved from IHC and the amount of protein in a cell is generally not linear[57]. A second disadvantage is that only one behavioural time point can be examined in each

animal, since they must be sacrificed to examine IEG expression. Thus, temporal changes in network activation can at best be inferred, and one must contend with the error associated with inter-experiment variability and not being able to examine network changes within the same animal.

In vivo imaging of IEGs

Capitalizing on the use of IEGs, researchers have developed transgenic animals that express fluorophores transiently in response to IEG gene activation. By implanting a cranial window in the skull of these animals, researchers can visualize cells that are active during a behavioural task by imaging the brain through the window. Importantly, the same ensembles of cells can be visualized over the course of many behaviour trials.

This approach was taken by Cao et al. (2015) using Arc-GFP (GFP: green fluorescent protein) mice[58]. The animals performed the rotarod task over the course of many days, and were imaged immediately after their training sessions to track the degree of activity in each cell of interest by measuring its fluorescence intensity. The results from this study showed that the level of fluorescence of each cell imaged during the rotarod training predicted whether it would be retained in the motor network used to perform the rotarod task or be dismissed. They also identified that the secondary motor cortex (M2) was required for motor learning.

This same approach can be taken without the use of IEG-driven fluorophores by substituting them for genetically encoded calcium indicators (GECIs). GECIs, such as GCaMP (and its variants), are a fusion protein of GFP and calmodulin, and have been used extensively to image populations of neurons during behavioural tasks[59]. During neural activity, calcium flows into the cell, and binds to the calmodulin portion of GCaMP, and a resulting conformational change causes the rapid deprotonation of the chromophore,

allowing for increased absorbance of the excitation wavelength and ensuing bright fluorescence. Given that intracellular calcium is rapidly chelated following neural activity, these rapid changes in intracellular calcium concentration cause signals to be perceived as a "flash" of fluorescence[59]. Thus, high temporal resolution can be achieved using GECIs. However, IEG-driven fluorophores and GECIs suffer from the same critical drawback. When performing *in vivo* imaging, one must choose to either image the whole brain at a superficial level using a CCD camera, or a smaller area of the brain with better depth and resolution with a two-photon microscope.

Inducible targeted recombination in active population (TRAP) models

Targeted recombination in active population (TRAP) models (not to be confused with "Translating Ribosome Affinity Purification") are inducible transgenic mice that allow for temporal and spatial examination of active cell ensembles at two time points within the same animal[60]. This is achieved via the combination of inducible IEG-driven fluorophore expression with IHC for IEGs. All TRAP models are double transgenic mice created by breeding together 1) an inducible Cre-estrogen receptor recombinase (CreER) mouse, in which the expression of Cre is under the control of an IEG promotor; and 2) a floxed STOP reporter mouse, in which the gene encoding a fluorophore is preceded by a STOP codon which itself is flanked by two LoxP sites (i.e. floxed). The CreER is a fusion protein of Cre recombinase and a mutated human estrogen receptor, whose activity is tamoxifen-dependent. In response to the binding of its ligand, tamoxifen, the CreER exposes its nuclear localization signal and translocates to the nucleus (Figure 1)[61]. When the CreER is in the nucleus, it cuts the DNA at the LoxP sites, thus excising the STOP codon and allowing for permanent expression of the reporter fluorophore only in cells that express CreER at the time of tamoxifen injection. Inducible TRAP models are unique in

that CreER expression is driven by that of IEGs[60]. Therefore, unlike traditional inducible models, CreER expression is 1) not limited to a specific type of neuron since it makes use of an IEG's promoter, and 2) transient, since it occurs only within a limited window of neuronal activity yet is able to permanently label active cells. As a result, this model can label networks active during behavioural tasks. The cells recruited to perform that task will

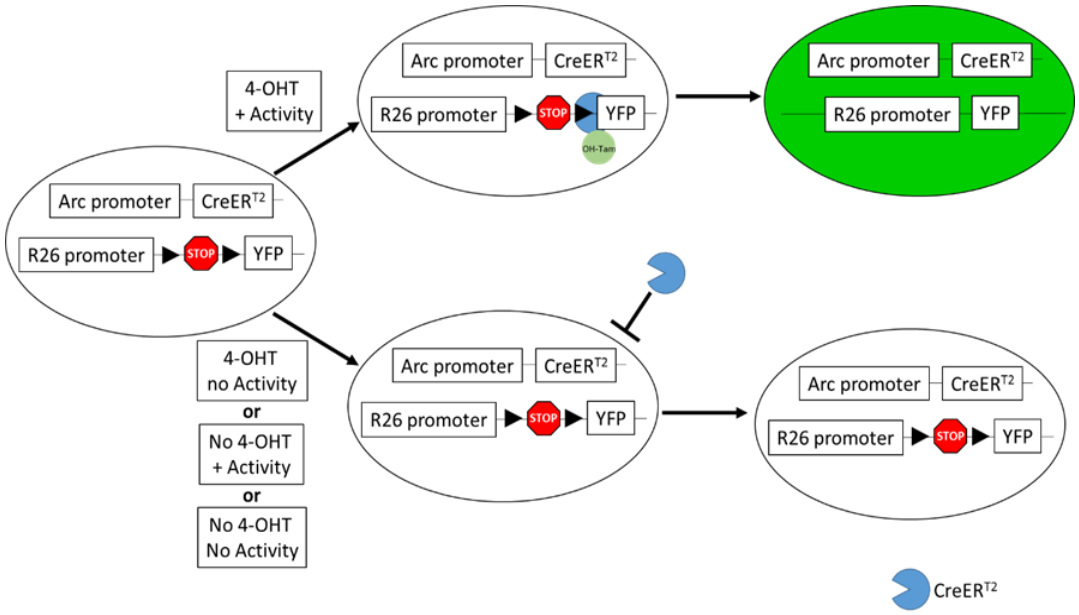

Figure 1: Labeling neuronal populations using the Arc-CreER^{T2}:YFP mouse. Neurons active during a behavioural task express Arc (and therefore CreER^{T2}). If OH-Tam is present while CreER^{T2} is available for recombination, the active cells will express YFP. If there is either no activity or no OH-Tam, the cells will not express YFP. Modified from Guenthner et al. (2013).

become active and express CreER, and if tamoxifen is present at this time, the cells will indelibly express the fluorophore. To date, three TRAP models have been created. Liqun Luo's laboratory at Stanford University created both a Fos-CreER^{T2} and Arc-CreER^{T2} mouse, and Rene Hen's laboratory at Columbia University created an Arc-CreER^{T2} mouse[60].

The first paper using a TRAP model was published in 2013 by Guenthner et al. (2013[62]). They created both a Fos-CreER^{T2} and Arc-CreER^{T2} mouse and demonstrated that

recombination in the primary somatosensory cortex, specifically the whisker barrel cortex, was sensory input-dependent. This was shown in an elegant experiment using two groups of mice. In one group, all but one whisker on the left side of the mice's faces were plucked which resulted in only one fluorescently-labeled whisker barrel. In the other group, only one whisker was plucked on the left side of the face which resulted in every whisker barrel, except the one corresponding to the plucked whisker being labeled. Using other modalities of sensory input, they also demonstrated substantially more recombination in response to stimulation and tamoxifen administration when compared to control groups that received only sensory stimulation or tamoxifen injection. In addition to these experimental controls, the authors compared the amount of tamoxifen-independent recombination between their two models. Surprisingly, they found some tamoxifen-independent recombination occurring in both the Fos-CreER^{T2} and Arc-CreER^{T2} mice, with more in the Arc-CreER^{T2}, which they suggested was due to Arc's higher level of baseline expression. They further showed that the administration of 4-hydroxytamoxifen (OH-Tam), the active form of tamoxifen, allowed for a much shorter labeling window when compared to tamoxifen. Finally, they demonstrated that these models are sensitive to labeling of hippocampal cells active during the exploration of novel environments. Thus, this paper provided strong support for the usage of these models for labeling populations activated during behaviour.

In 2014, Rene Hen's group published their own Arc-CreER^{T2} mouse in two high impact publications[63,64]. Denny et al. (2014[63]) found that the strength of fear memories can be predicted based on the degree of reactivation in the hippocampal dentate gyrus (DG) and Cornu Ammonis region 3 (CA3). Later that year, Root et al. (2014[64]) used this mouse to investigate the pathways involved in odour discrimination[64]. Similar to the findings by

Guenthner et al. (2013[65]), Denny et al. (2014[63]) found that mice treated with OH-Tam increased the specificity of cells labeled when compared to tamoxifen[63]. To determine the functional role of the active cells in learning, both papers used a novel approach of combining their Arc-CreER^{T2} mice with the use of optogenetics. Specifically, they crossed their Arc-CreER^{T2} mice with either floxed-STOP-Archaerhodopsin-3-GFP (Arch) or floxed-STOP-ChR2-YFP mice. This allowed Denny et al. to selectively silence (with Arch) or activate (with ChR2) neuronal populations that are recruited during a fear conditioning task by shining light through a fiber optic wire into the hippocampal dentate gyrus (DG) or Cornu Ammonis region 3 (CA3)[63]. It also allowed Root et al. to silence the pathways involved in discriminating between aversive or appetitive odours[64]. These high-impact results demonstrated the strength of this system to reliably target specific populations of neurons and advanced the field by combining TRAP models with optogenetics to influence the activity of cells recruited during a behavioural task. These models have since been used to investigate memory decline in Alzheimer's disease[66].

Following the publication of these seminal findings, these models have provided insight into and investigated the cellular populations of the prefrontal cortex associated with appetitive (cocaine) and aversive (shock) stimuli. Most recently, using the TRAP models developed in Liqun Luo's laboratory, Ye et al. (2016[67]) combined TRAP approaches with CLARITY in order to demonstrate at a whole-brain level the cells recruited by each stimulus, and most importantly, the other brain locations to which they connected. Together, these publications strongly support the strength and utility of TRAP models. These models are enticing for work in stroke recovery, since the populations of

neurons recruited at various times during the process of recovery can be labeled and stimulated optogenetically.

2. Aims and hypotheses

Aims

1) To establish a model in which cells active during a behavioural task at two separate time points can be labeled.
2) Evaluate the effect of stimulating contralesional motor cortex cells recruited to perform a behavioural task on stroke recovery.

Hypotheses

1) We hypothesize that the Arc-CreER^{T2} mouse will reliably label cells motor cortex cells recruited to perform a behavioural task.
2) We hypothesize that contralesional activation of motor cortex cells recruited to perform a behavioural task will impair recovery after stroke.

3. Methods

Animals

All animals were bred and housed in the University of Ottawa Animal Care and Veterinary Services facility. Both the Arc-CreER^{T2}:Rosa-YFP$^{f/f}$ and the Arc-CreER^{T2}:Rosa-ChR2:YFP$^{f/f}$ breeding pairs were previously published and gifts from our collaborator, Dr Christine Denny[63]. After weaning animals were group-housed on a 12-hour light cycle (lights on at 7:00 EST, lights off at 19:00 EST). Animals had food and water available *ad libitum*. The temperature and humidity in the housing room was kept at 23°C and 28%, respectively. All animal procedures were conducted with the approval of the University of Ottawa's Animal Care Committee and in accordance with guidelines set out by the Canadian Council of Animal Care.

For the motor network labeling experiments presented in Chapter 1, the experimental mice (10-12 weeks old) were heterozygous for Arc-CreER^{T2} and Rosa-YFP$^{f/f}$. The mice were individually housed one week prior to behavioural testing. For the *in vivo* optogenetic experiments presented in Chapter 2, the mice were all heterozygous for Arc-CreER^{T2} and Rosa-ChR2:YFP$^{f/f}$. Animals were individually housed immediately following optic fiber implant surgery.

Behaviour

Adhesive removal: The adhesive-removal task is an assessment of sensorimotor function[68]. Briefly, mice are placed into an empty cage for one minute, and then a 3x3 mm piece of tape is placed on each one of their paws. The time it takes for the mouse to contact and remove each one of the pieces of tape is recorded. The animals have a maximum of two minutes to remove both pieces of tape. If they fail to do so during the training phase,

the tape is left on. If they fail to remove the tape during any of the post-stroke testing days, it is removed from their paws before they are returned to their home cage. Animals were trained once per day for five days. Training and testing took place in the morning.

Rotarod: The rotarod test is used as an assessment of motor ability including motor learning and gross limb coordination[69]. The rotarod was used in these experiments as a method to induce robust activation in the primary and secondary motor cortices, as previously published using the Arc-GFP mice[58,70]. During this task, mice were placed on the rotarod (Med Associates) that was set to rotate at 2 revolutions per minute (RPM). The speed of the rod increased to 20 RPM within one minute. The test was ended when either two minutes expired, or the mice fell off the apparatus. The mice landed on a metal plate, which then triggered the apparatus to stop and record the time at which the mouse fell. Mice were exposed to the rotarod 10 times per session, with no intertrial interval.

Cylinder: The cylinder task is an assessment of spontaneous forelimb use[71] and was used for the stimulation experiments in Chapter 2. It involves placing the mouse in a 10-centimetre glass beaker and, as it rears, observing how much time it spends using each one of its forepaws to support itself. Ethovision XT 11 was used to record, and The Observer XT 13 was used to score the data (Noldus).

OH-Tam treatment

Three different OH-Tam treatment protocols were utilized in experiments within this thesis and are described in detail within the results section. To reduce the stress associated with intraperitoneal injection, mice were handled and injected with sterile normal saline once per day for 5 days, one week prior to start of the experiment.

OH-Tam delivered in oil (two mg per animal): OH-Tam was prepared in oil and administered as previously described[63]. Briefly, a 10 mg/mL solution of OH-Tam was prepared by first dissolving OH-Tam powder (H6278; Sigma) in 100% ethanol (EtOH), and then in corn oil. Pinpoint sonication was used to ensure a complete dissolution (70% power, 1 minute total time, 10 seconds on, 5 seconds off). Each animal, regardless of weight, received 200 μL of prepared OH-Tam solution (2 mg). Animals were placed into a dark room for one day prior to OH-Tam injection. Five hours after OH-Tam injection, animals were exposed to a behavioural task to label the recruited networks. Animals were left in the dark room for two days after behaviour to ensure minimal background labeling[63].

OH-Tam delivered in saline (5 mg/kg): OH-Tam was prepared in DMSO and saline as previously described[67]. Briefly, a 1 mg/mL solution of OH-Tam was prepared by first dissolving OH-Tam in dimethyl sulfoxide (DMSO, D5879; Sigma), then polyoxyethylenesorbitan monolaurate (Tween-20, P9416; Sigma). The final solution contained 1 mg/mL OH-Tam, 2.5% DMSO, and 1% Tween-20 dissolved in sterile 0.9% saline. Each animal received 5 mg of OH-Tam per kg body weight. Animals were placed into a quiet room with normal light cycle the day before OH-Tam injection to ensure minimal background activation. Animals were injected with OH-Tam three hours post-behaviour, left in the room overnight, and returned to their housing room the next morning.

OH-Tam delivered in saline (40 mg/kg): OH-Tam was also prepared at a higher concentration than previously described. A 2.5 mg/mL solution of OH-Tam was prepared by first dissolving OH-Tam in DMSO, then Tween-20. The final solution contained 2.5 mg/mL OH-Tam, 2.5% DMSO, and 2% Tween-20 dissolved in sterile 0.9% saline. Each animal received 40 mg of OH-Tam per kg of body weight. Animals were placed into a

quiet room with normal light cycle the day before OH-Tam injection to ensure minimal background activation. Animals were injected with OH-Tam either three hours post-behaviour, left in the room overnight, and returned to their housing room the next morning.

Photothrombosis surgery

Ischemia was induced in the motor cortex of mice using the previously-described photothrombosis stroke model[72]. Briefly, mice were anesthetized with 5% isoflurane and 1% oxygen, and placed under a heat lamp. Animals were given an injection of Rose Bengal (10mg/ml, R3877-5G; Sigma) and mounted into the stereotaxic frame. The skull was exposed, and the stroke coordinates were measured relative to Bregma (0.7 AP, +1.5 ML, 3 cm laser height). Five minutes after the Rose Bengal injection, a green laser (532 nm, 25 mW, MGM20; Beta Instruments) was used to irradiate the brain for ten minutes. After irradiation, the scalp was closed with tissue glue, and 2% bupivacaine was administered as an analgesic. Body temperature was maintained between 36.5 and 37.5 °C using a rectal temperature probe attached to a feedback heating blanket (Harvard Apparatus).

***In Vivo* optogenetics apparatus**

Optic fiber implant surgery: Fiber optic implants were stereotaxically implanted into the motor cortex by Anthony Carter (Canadian Partnership for Stroke Recovery) and David Lemelin (then-Béïque lab member). After anesthesia, animals were mounted onto a stereotaxic frame and two holes were drilled, one at M1 (Bregma 0.7 AP, -1.5 ML, -0.5 DV) for the fiber optic implant, and another 2 mm posterior to the first for the skull screw (B002SG89KW; Antrin Miniature Specialties). After lowering the implant and skull screw into the skull, the base of the implant and entire skull screw were covered in dental cement (431011; GC America). Once the dental cement had dried, the skin was sealed with tissue

glue (Vetbond, 084-1469SB; 3M), and transdermal bupivacaine was applied to the incision.

Fabrication of optogenetic implants and patch cords: The implants consisted of a 100 μm fiber optic wire in a 110 μm ceramic ferrule, with the fiber optic wire protruding from one end of the ferrule. 100 μm fiber optic wire (FG105LCA; Thorlabs) was stripped and cut to a length of 7.5 mm. This allowed for 0.5 mm to protrude from the end of a 100 μm ceramic ferrule (MM-FER2007C-1270; PFP). Epoxy (F120; Thorlabs) was applied to the implant and allowed to cure for two days before polishing. Patch cords were made in a similar way. After stripping both ends of a 60 cm section of 200 μm fiber (FG200LEA; Thorlabs), a 200 μm ceramic ferrule (MM-FER2007C-2300; PFP) was placed onto one end, and a LC connector and white boot were placed on the other (MM-CON2007-2300-9-WHT; PFP). Implants and patch cords were polished using four calcined alumina polishing sheets of increasingly fine grit (all from Thorlabs: 5 μm grit; LF5P, 3 μm grit; LF3P, 1 μm grit; LF1P, and 0.3 μm grit; LF03P). A polishing disk (M1-80754; PFP) and polishing pad (M1-46165; PFP) were used to ensure that implants did not break during the polishing process. Implants and patch cords were tested using a power meter (PM20A; Thorlabs) to ensure consistency of light delivery across animals.

Optogenetic stimulation

Optogenetic stimulation was delivered using a light generation system. This system consisted of a computer running the Radiant software (Plexon), which communicated the frequency and intensity instructions to an optical driver (PlexBright, Plexon). The optical driver in turn was routed to a commutator (PlexBright Dual LED Commutator; Plexon), to which a blue LED was connected (465 nm, PlexBright Head-Mounted LED Module;

Plexon). A patch cable was then used to deliver light from the LED to the fiber optic implant, and into the brain to activate ChR2. A split sleeve (SM-CS125S; PFP) was used to connect the patch cord to the implant.

Mice were lightly anesthetized with 4% isoflurane before patch cords were connected to their implants. Mice were stimulated in the morning, and at least four hours prior to any behavioural test. After receiving optogenetic stimulation, animals were anesthetized once again, and the patch cords were disconnected from their implants.

Transcardial perfusion

Ninety minutes after behaviour or optogenetic stimulation, animals were deeply anesthetized with 0.1 mL of sodium pentobarbital (Euthanyl, 65 mg/mL), and perfused for six minutes with 1X phosphate-buffered saline (PBS), and then for 10 minutes with 4% paraformaldehyde (PFA) in 1X PBS (both 4°C, pH 7.4, 7 mL/minute). Brains were removed and post-fixed in 4% PFA for one hour, and cryoprotected in 30% sucrose with 0.1% sodium azide (NaN_3, 71290; Sigma) until sectioning.

Immunohistochemistry

Brains were sectioned at a thickness of 40 µm using a freezing microtome (SM 2010R; Leica) and placed serially into nine wells filled with 1X PBS with 0.1% NaN_3. All sections were taken out of the PBS+NaN_3 solution and rinsed three times in 1XPBS. Sections were then put into blocking solution for one hour. The blocking solution contained 3% normal donkey serum (NDS, 017-000-121; Jackson ImmunoResearch) in free-floating (FF) carrier solution. The FF carrier was made of 0.1% Triton X-100 (BP151500; Fisher) and 0.1% Tween-20 in 1XPBS. After blocking, solutions were transferred into primary

antibody solutions (appropriate primary antibodies and 3% NDS in FF carrier) for 24 hours at 4 degrees Celsius with gentle shaking. Primary antibody concentrations were: 1:5000 for chicken α-GFP (for YFP, GFP-1020; Aves), 1:5000 for rabbit α-c-Fos (226 003; Synaptic Systems), 1:1000 for guinea pig α-Arc (156 005; Synaptic Systems).

The following day, all sections were rinsed three times in 1XPBS for five minutes and incubated with secondary antibodies (all 1:500, from Jackson ImmunoResearch) and protected from light with tin foil. Antibodies used were AlexaFluor 488 α-rabbit (711-545-152), CY3 α-chicken (703-165-155), CY3 α-guinea pig (706-585-148). After secondary antibody incubation, sections were rinsed three times in 1XPBS for five minutes, and incubated for five minutes with 4',6-diamidino-2-phenylindole (DAPI, nuclear counterstain, 10236276001; Sigma). Sections were then rinsed three more times, mounted onto charged SuperFrost Plus slides (Fisher, 1255015), and coverslipped with #1 coverslips (12-545M; Fisher) and ImmuMount mounting medium (2860060; Fisher).

Acquisition of images and quantification of YFP+ and c-Fos+ cells

A modified version of the protocol set out in Muñoz et al. (2017) was followed to quantify the number of YFP+ and c-Fos+ cells in the motor cortices[73]. Every ninth section throughout the caudal forelimb area (AP +1.0 to 0, relative to Bregma) was examined. In total, three sections from each animal was examined. In each section, the upper and lower parts of the M1 and M2 cortices were scanned using an epifluorescent microscope at 20x magnification (Zeiss, AxioImager M2). Twenty-four images were taken for YFP and c-Fos analysis (three sections per animal, upper and lower M1 and M2 on both sides of the brain). M1 and M2 were defined according to the Paxinos and Watson Brain Atlas. Briefly, M2 was defined as 0.5 mm from the midline, and M2 was defined as 1.5 mm from the midline,

and immediately lateral to M2. The upper layers were defined as layers 1 and 2-3, and the lower layers were defined as layers 5A, 5B, and 6. Optical sectioning was performed using the Apotome.2 attachment (Zeiss). Images were deconvolved using default settings in the Zen Blue software (Zeiss). Three-dimensional images were loaded into Imaris 9 (Bitplane). YFP+ (average size 15 μm) and c-Fos+ (average size 10 μm) cells were detected automatically. After manual corrections were applied to the automatic cell detection, the distance between the YFP and c-Fos cells was set to 7 μm.

Quantification of Arc+ and c-Fos+ cells

One representative image from lower M1 in the most anterior section was used to quantify the number of c-Fos+ and Arc+ cells throughout the entire section. Using Zen, cells were identified as either Arc+, c-Fos+, or Arc+ and c-Fos+.

Lesion volume analysis

All sections with ischemic damage were mounted onto SuperFrost Plus charged slides and allowed to dry for 12-14 hours. Slides then underwent the following steps to visualize stroke damage. Slides were dehydrated in: 1) 70% EtOH for 10 dips, 2) 95% EtOH for 20 dips, 3) 100% EtOH for 20 dips. Slides were then rehydrated by proceeding in the reverse order of the dehydration: 4) 95% EtOH for 20 dips, 5) 70% Ethanol for 10 dips, 6) MQ H_2O for 1 minute. After rehydration, the slides were stained in 0.25% cresyl violet acetate (0.25% cresyl violet dissolved in Acetate Buffer (0.5% sodium acetate, 0.003% acetic acid, 1.4% ethanol in distilled H_2O) pH 4.0): 7) Cresyl violet for 6-7 minutes, 8) MQ H_2O for 10 dips, 9) 70% EtOH for 10 dips, 10) 95% EtOH for 10 dips. Slides then underwent differentiation: 11) 0.25% glacial acetic acid in 100% EtOH for 6 dips, 12) 95%

EtOH for 10 dips, 13) 100% EtOH for 10 dips. Finally, slides were immersed in clearing agent (Citrisolv, 22-143-975; Fisher), to remove of any remaining residue: 14) Citrisolv for 1 minute, 15) Citrisolv for 3 minutes. Slides were then coverslipped with DPX mounting media (44581; Sigma) and left to dry overnight

Statistical Analyses

All statistical analyses were performed in Prism 6 (GraphPad). Analysis of two independent groups was done using an unpaired t-test, dependent groups were analyzed using a paired t-test. Bivariate data was analyzed using a two-way analysis of variance with repeated measures used when indicated. Multiple comparisons were done using a Holm-Šidák test. Family-wise type 1 error was set at $\alpha=0.05$.

4. Results

Aim 1: Using the Arc-CreER^{T2}:YFP mouse to identify cells in the motor cortex that are active during SBR.

Is labeling in the motor cortex of Arc-CreER^{T2}:YFP$^{f/f}$ mice OH-Tam-dependent?

To determine the networks recruited during a motor task, Arc-CreER^{T2}:YFP$^{f/f}$ mice[63] were acquired from our collaborator, Dr. Christine Denny, at Columbia University (New York, NY). To confirm that YFP+ expression was OH-Tam-dependent, mice performed the adhesive removal task in the presence or absence of OH-Tam treatment. This task was chosen because it is a well-validated sensorimotor task[68] and, in the long term, we wished to label the cells recruited at various time points up to 90 days post-stroke[72].

The timeline for this experiment is shown in Figure 2A. This experiment made use of the procedures developed by Denny et al. (2014[63]). Individually-housed mice began bilateral training on the adhesive removal task once per day for five days prior to labelling. During this time, animals improved both their time to contact and remove the tape (Figure 2B-C).

Two days after the last day of training, mice were placed into a dark room to mitigate the risk of non-task-related recombination. The next day, half of the mice were given an injection of OH-Tam. Five hours later, all mice performed the adhesive removal task with one paw to elicit activation of the motor cortices. Mice were left in the dark for two days after OH-Tam injection to again mitigate the risk of non-task-related recombination. As shown in Figure 2D, those that received a vehicle injection had negligible amounts of staining, (<5 YFP+ cells in the motor cortices). Only animals that

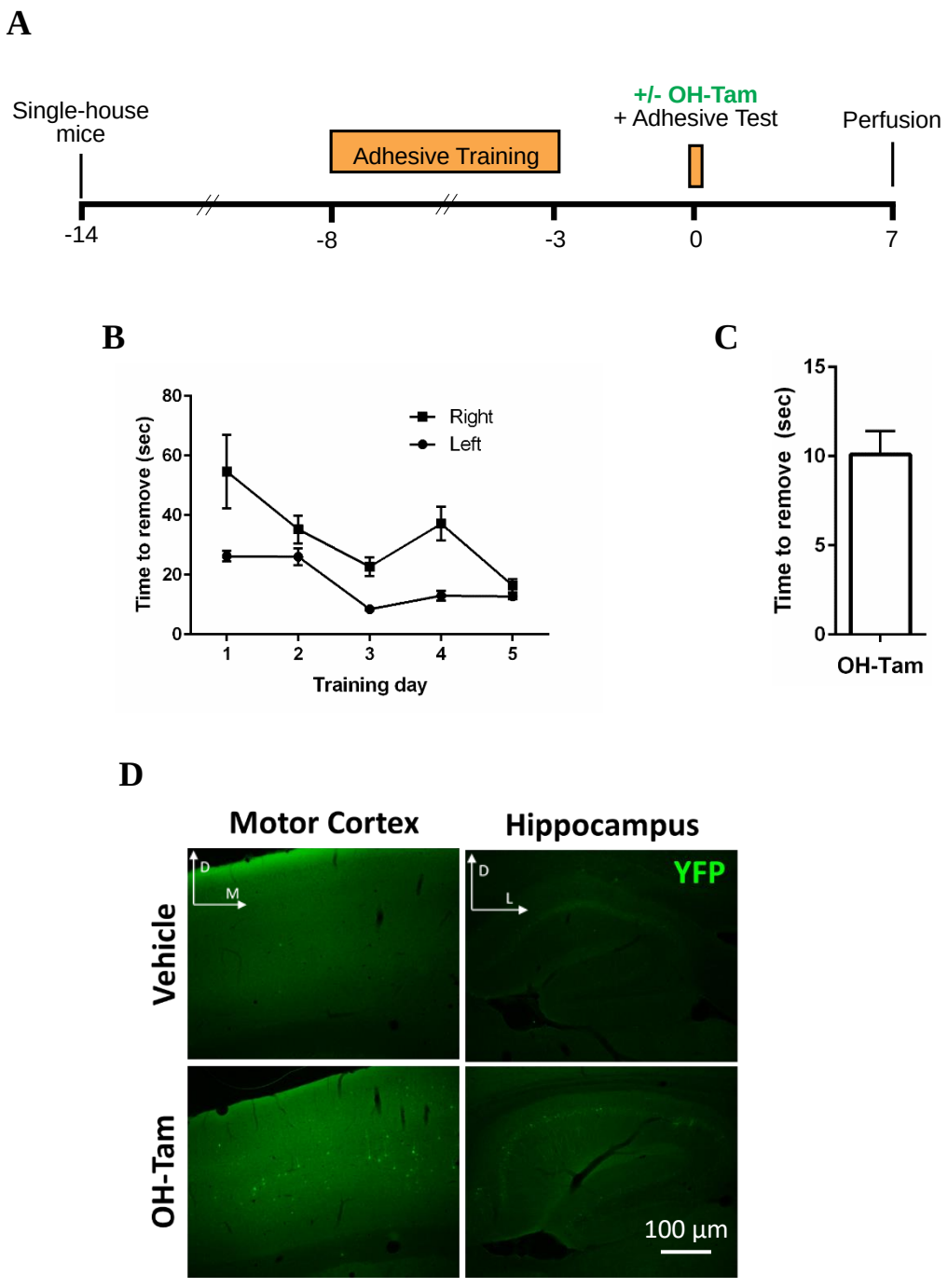

Figure 2: Labeling in the ArcCreER^{T2}:YFP mouse is OH-Tam dependent. **A** Experimental timeline. **B** Adhesive removal training. **C** Adhesive removal performance on day of OH-Tam injection. **D** Representative images of YFP labeling in the cortex and hippocampus.

received OH-Tam had substantial amounts of labeling. This confirmed the results from previous studies showing that labeling in these models is OH-Tam-dependent[63-65]. It also suggested that the adhesive task can be used for labeling ensembles in the motor cortex.

Does performing the adhesive task produce activity-dependent labeling in the motor cortex?

The next step in validating the reliability of motor cortex labeling in the Arc-CreER^{T2} mouse model was to determine whether YFP expression was dependent on the animals performing the adhesive task. The design of this experiment was similar to the one described in Figure 2A, except all animals received OH-Tam, and mice were randomly assigned to either perform the adhesive removal task or remain in their home cage (Figure 3A). During adhesive training, mice reduced their time to remove the tape from their paw (Figure 3B). As expected, following OH-TAM injection mice quickly contacted and removed (average 15 seconds) the tape (Figure 3C).

Surprisingly, the analysis of the YFP+ cells revealed that in both animals performing the adhesive removal task and home cage controls showed a high degree of variability in the number of YFP+ cells in the motor cortex (Figure 3D). It was expected that YFP expression in the motor cortex would be greater in the animals that performed the adhesive task than in the ones left in their home cage. One possible reason this occurred was that this labeling paradigm is unable to distinguish between cells activated by performing the adhesive task and those activated during home cage behaviours, such as walking, grooming, or eating. We therefore sought to increase the labeling specificity in our model by increasing the "signal-to-noise ratio" of the labeling in this model. We hypothesized this could be accomplished by "increasing the signal" in this system by

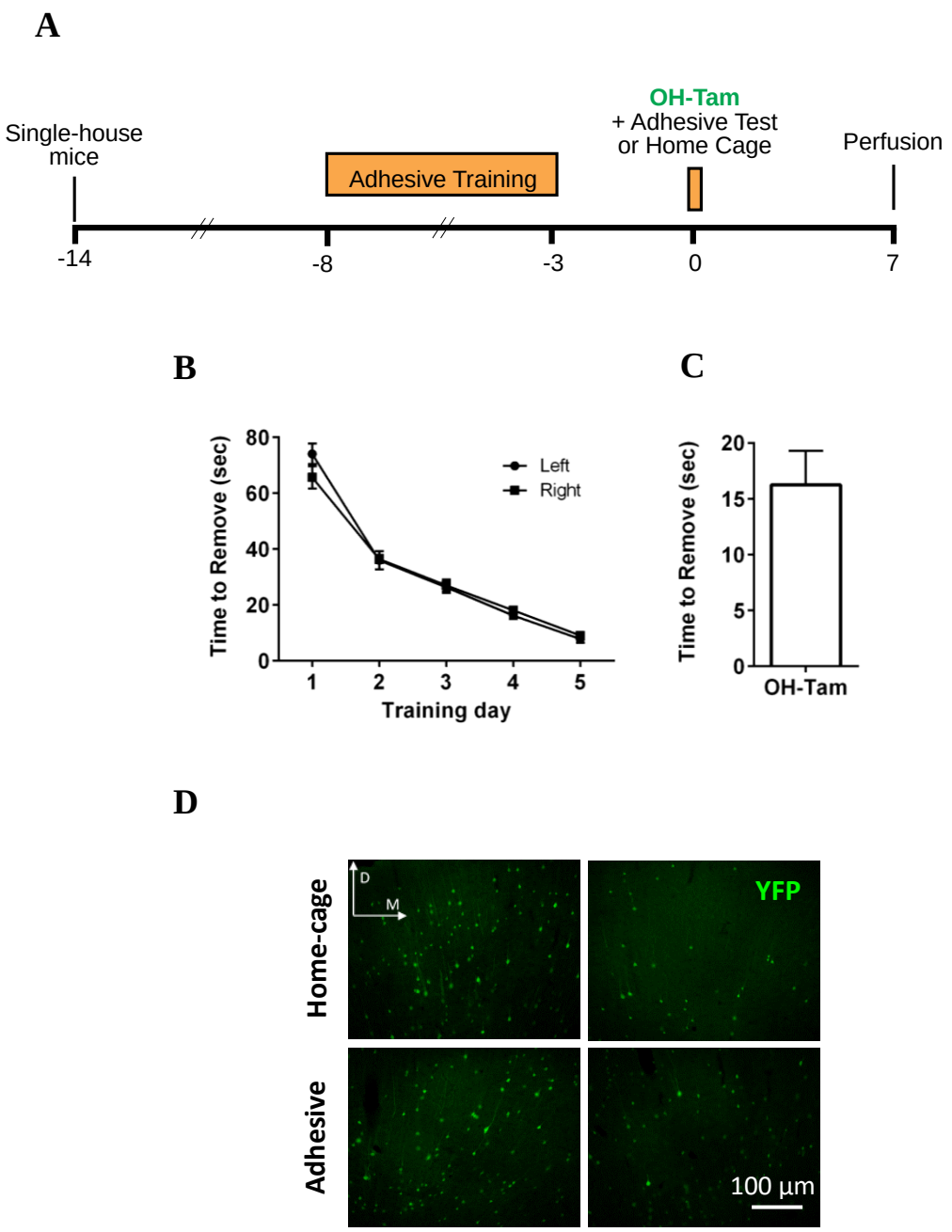

Figure 3: The adhesive removal task does not result in specific labeling of cortical neuronal populations when used in conjunction with the OH-Tam dissolved in EtOH and oil. **A** Experimental timeline. **B** Adhesive removal training. **C** Adhesive removal performance on day of OH-Tam injection. **D** Representative images of YFP labeling in the motor cortex.

having the animals perform a task which elicits greater activity in the motor cortex to increase the number of YFP+ cells recruited by the behavioural task. Alternatively, "decreasing the noise" in this system would result in greater degree of task-specific labeling by reducing the number of YFP+ cells captured by home cage activation. This could be achieved by shortening the labeling window.

Does performing the rotarod task increase labeling specificity in the motor cortex?

To increase the signal, we examined whether rotarod performance would induce greater YFP labeling than the adhesive removal task. The rotarod task seemed like an ideal task, since it has been previously shown to elicit strong activation in the motor cortices and has been used in previous studies of motor behaviour[58,70].

The timeline for this experiment is shown in Figure 4A. One week after being individually-housed, animals were pre-trained on the rotarod. The protocol for the rotarod included 10 trials, with no inter-trial interval, as the animals were immediately placed back onto the rotarod after they had fallen off (Figure 4B-D). After pre-training, mice were left in a dark room. The next day, animals were given an injection of OH-Tam, and five hours later exposed to the rotarod. Rotarod performance during pre-training and on the day of OH-Tam were similar (Figure 4 E-G).

Mice were left in the dark for two days after the day of OH-Tam injection. Mice were sacrificed one week after OH-Tam injection for examination of YFP+ cells. Quantification of the number of YFP+ cells revealed no difference between animals exposed to the rotarod and those that remained in their home cage (Figure 5). Given that we did not observe any obvious difference in YFP labeling between home cage controls

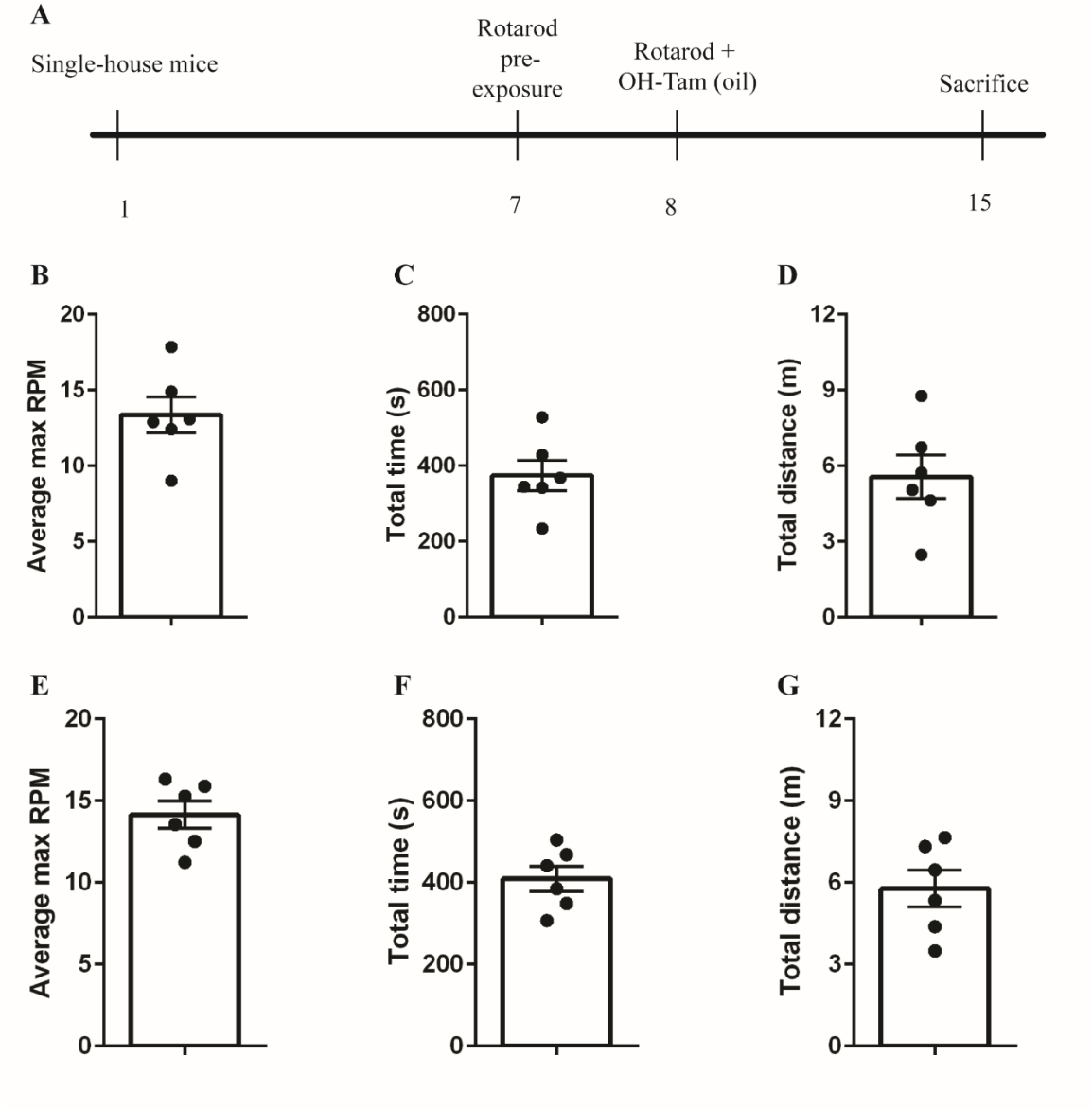

Figure 4: Labeling of networks active during rotarod using OH-Tam dissolved in oil. **A** Timeline of experiment. Rotarod performance during pre-training: **B** average maximum rotation speed; **C** time; **D** distance traveled. Rotarod performance on day of OH-Tam injection: **E** average maximum rotation speed; **F** time; **G** distance traveled. Error bars represent SEM.

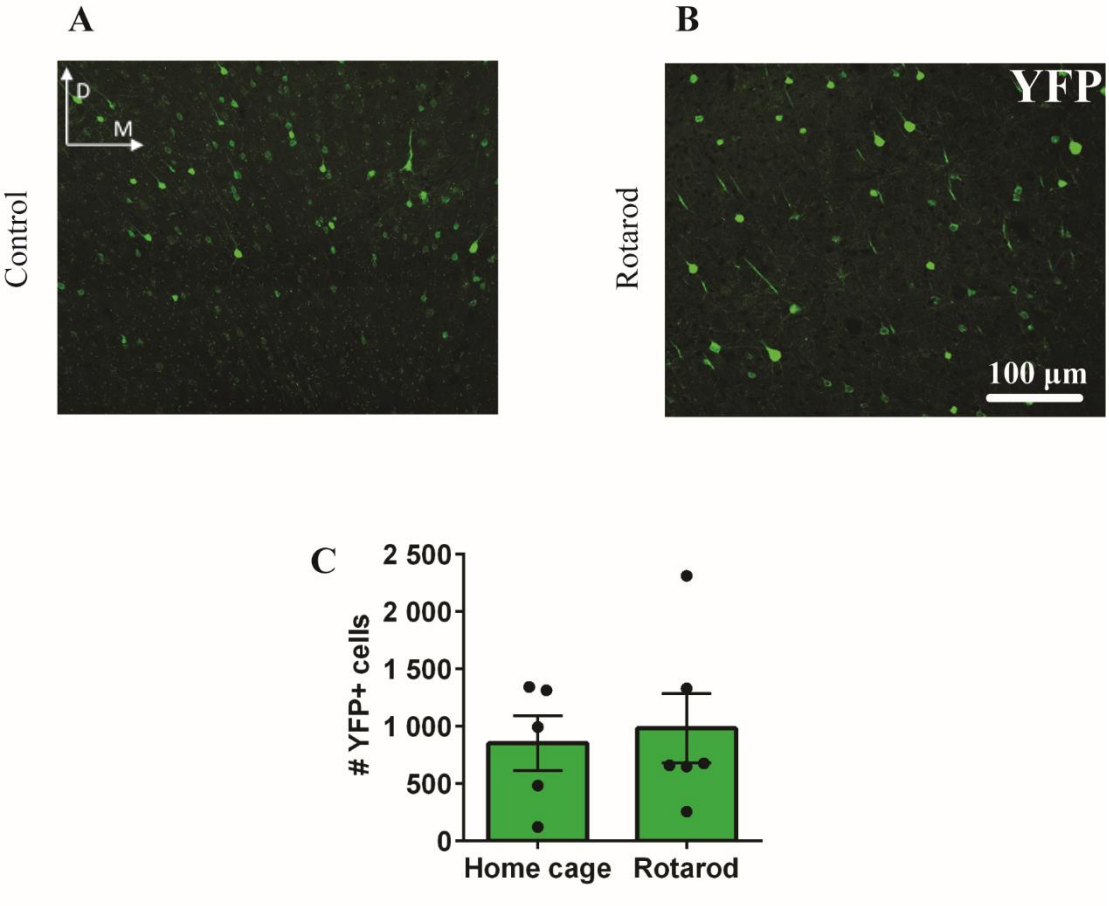

Figure 5: Quantification of cells labeled during rotarod using OH-Tam dissolved in oil. Sample images: **A** home cage controls; **B** rotarod animals. **C** Quantification of labeled cells. Error bars represent SEM.

and rotarod animals, we decided not to proceed with the quantification of c-Fos+ or colabeled cells.

This result suggested that using rotarod, a task which takes longer to perform and has been shown to be IEG-dependent[70], was insufficient to achieve specific labeling. This result also led us to believe that perhaps decreasing background activation by altering the OH-Tam treatment paradigm may be required.

Does increasing the activity in the motor cortex and reducing the labeling window result in specific labeling?

To reduce the amount of background activation captured by our YFP labeling, we sought to shorten the window during which OH-Tam is bioavailable. To accomplish this, we made use of a protocol published in a paper by Ye et al. in late 2016. In this paper, the authors put forth a method of dissolving and administering OH-Tam so that the drug was only bioavailable for one to two hours. This labeling window was much shorter than the six-hour window achieved when dissolving OH-Tam in oil and ethanol[67,74].

The timeline for this experiment is in Figure 6A. For this experiment, animals were put through the same experimental plan as the previous experiment, except that OH-Tam was delivered in DMSO and saline three hours post-rotarod, and the animals were left on a regular light cycle. Rotarod performance was similar between pre-exposure, the day of OH-Tam, and the day of sacrifice (Figure 6B-G). Analysis of the YFP+ cells also showed that the animals exposed to the rotarod showed a trend toward an increase in the number of YFP+ cells (Figure 7). This suggests that using this formulation of OH-Tam is capturing less background activity and can therefore differentiate between animals that remained in their home cage and those that performed rotarod. However, when YFP counts were

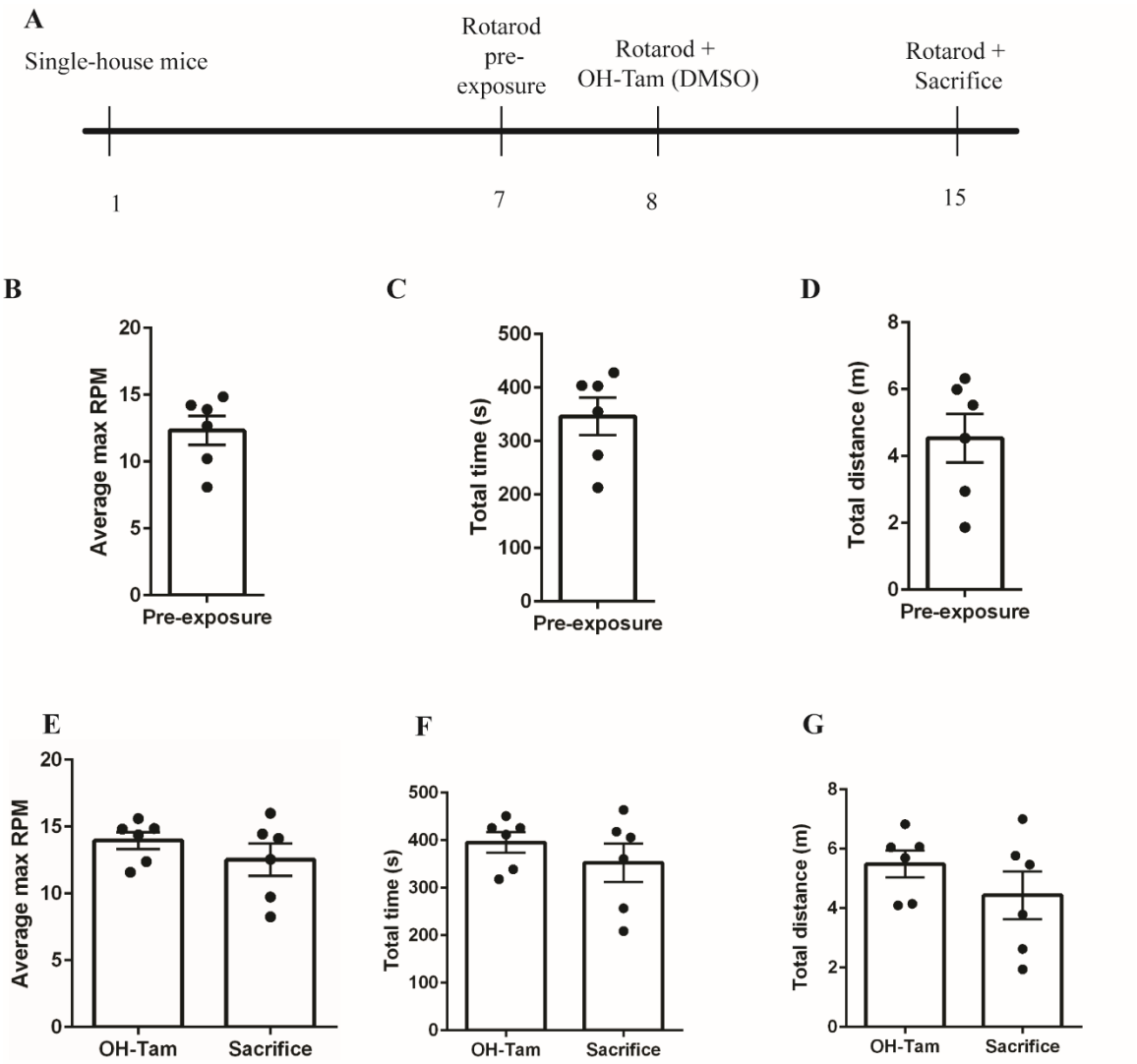

Figure 6: Labeling of networks active during rotarod using OH-Tam dissolved DMSO and saline (5 mg/kg). **A** Timeline of experiment Rotarod performance during pre-training: **B** average maximum rotation speed; **C** time; **D** distance traveled. Rotarod performance on day of OH-Tam injection and sacrifice: **E** average maximum rotation speed; **F** time; **G** distance traveled. Error bars represent SEM.

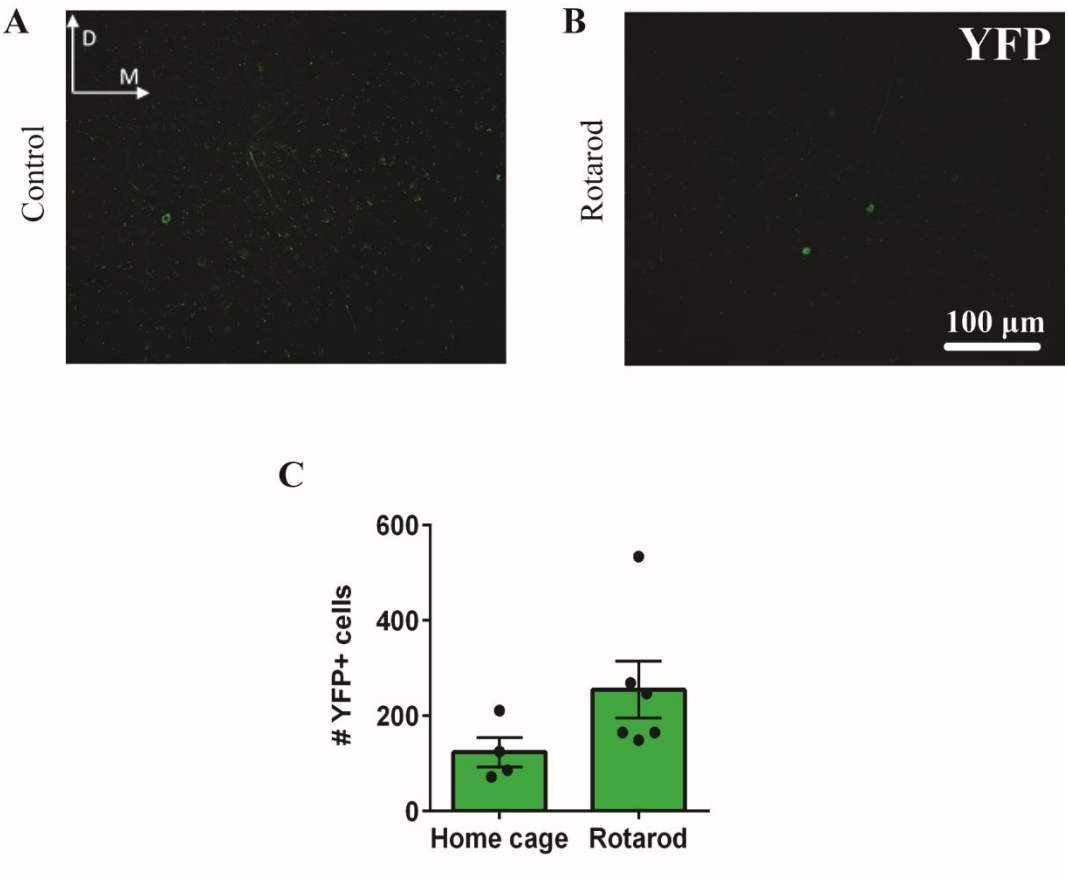

Figure 7: Quantification of YFP+ cells labeled during rotarod using OH-Tam dissolved in DMSO and saline (5 mg/kg). Representative images: **A** home cage; **B** rotarod animals. Quantification of YFP+ cells ($t=1.681$, $df=8$, $p=0.1314$). Error bars represent SEM.

compared to those of the previous experiment (Figure 5), it appeared that the animals that received this new formulation of OH-Tam had significantly fewer YFP+ cells than their counterparts who received OH-Tam delivered in oil. This could be because the labeling window was shortened, but also because the dose of OH-Tam for this experiment was five mg/kg, as opposed to two mg (80 mg/kg in a 25 g mouse) used when delivering the OH-Tam in oil.

Can c-Fos be used as a marker of active cells at the second behavioural time point?

Previous studies using TRAP mice have used endogenous Arc protein as a marker of active cells at the sacrifice behavioural time point[63,67]. However, since Arc mRNA has been shown to be translated locally at synapses in response to synaptic activity (making it difficult to colabel with our somatic YFP marker), and Arc mRNA has also been shown to be shuttled between neighboring cells, we sought to use another marker of cellular activity at the sacrifice time point[62,75,76]. The IEG c-Fos has been previously shown to have similar activation and degradation kinetics to Arc protein[55]. To determine whether c-Fos was a suitable proxy for Arc, we sought to quantify the overlap in Arc and c-Fs expression.

As shown in Figure 8A, in this experiment the animals were pre-exposed to the rotarod, and the next day re-exposed to the rotarod and sacrificed 90 minutes later. On average, mice remained on the rotarod for a total of six metres (Figure 8B). Immunohistochemistry revealed that over 95% of the cells that expressed c-Fos also expressed Arc. Similarly, over 95% of the cells that expressed Arc also expressed c-Fos (Figure 8C and D). This finding confirms previous reports[62,63], and thus all subsequent analyses of cells active at our second behavioural time point will be done using c-Fos.

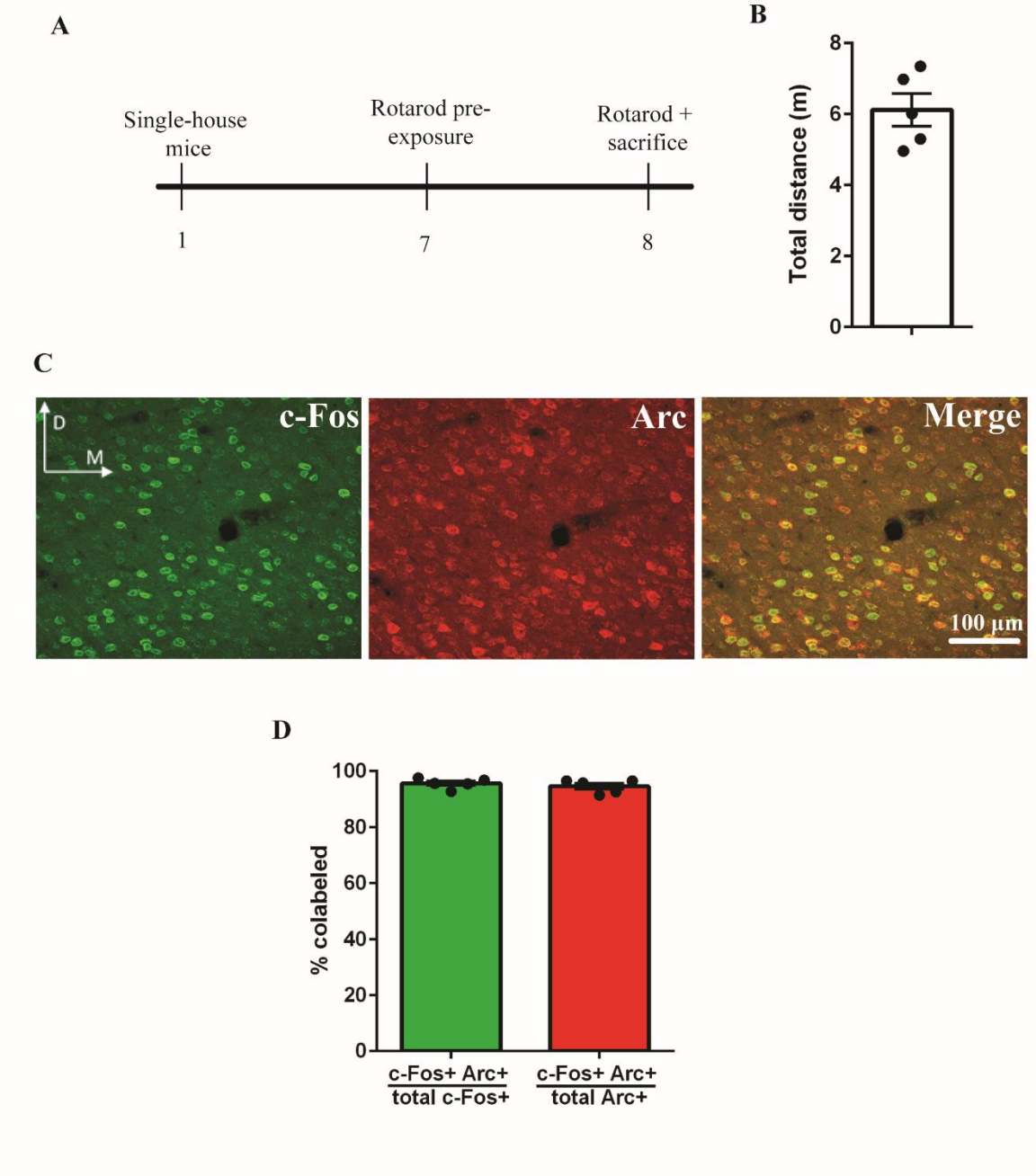

Figure 8: Colocalization analysis of c-Fos and Arc. **A** Timeline of experiment. **B** Distance traveled on the rotarod before sacrifice. **C** Representative image of c-Fos and Arc staining. **D** Percentage of c-Fos+ cells that were also Arc+ (green) and Arc+ cells that were also c-Fos+ (red) (t=1.528, df=4, p= 0.2012) . Error bars represent SEM. Data analyzed using a parametric paired t-test.

Do cells colabel when performing rotarod one week apart?

Using the same animals as used in Figures 6 and 7, we sought to examine whether animals that performed rotarod at the time of sacrifice had more c-Fos+ cells than home cage controls. Indeed, rotarod animals had significantly more c-Fos+ cells in their motor cortices than home cage controls (Figure 9). The comparison of the number of colabeled YFP+ c-Fos+ cells (Figure 10) between home cage control and rotarod animals did not yield a significant difference. However, the home cage control animals showed less variability in both measures.

Both groups had similar percentages of YFP+ cells that were also c-Fos+ (Figure 10D, YFP+ c-Fos+/ total YFP+). This percentage is also in alignment with the amount of reactivation observed in the original paper in which this method was published[67]. Since previous work using rotarod had demonstrated region specific activation, we too sought to separate our analyses by area (Figure 11). Specifically, it appeared that the large increase in c-Fos+ cells in rotarod animals was due primarily to an increase in c-Fos+ cells in the upper M1 and M2.

We noticed that the number of YFP+ cells labeled using the paradigm published by Ye et al. (2016[67]) was much lower than the number of cells recruited when using OH-Tam delivered in the way described by Denny et al. (2014[63]) This was most likely due to the difference in dose between the two paradigms. In this publication, the authors used two mg of OH-Tam per animal (80 mg/kg in a 25 g mouse), whereas the paradigm published by Ye et al. used five mg/kg. We hypothesized that we could increase the number of cells labeled with YFP by simply increasing the dose of OH-Tam delivered in saline.

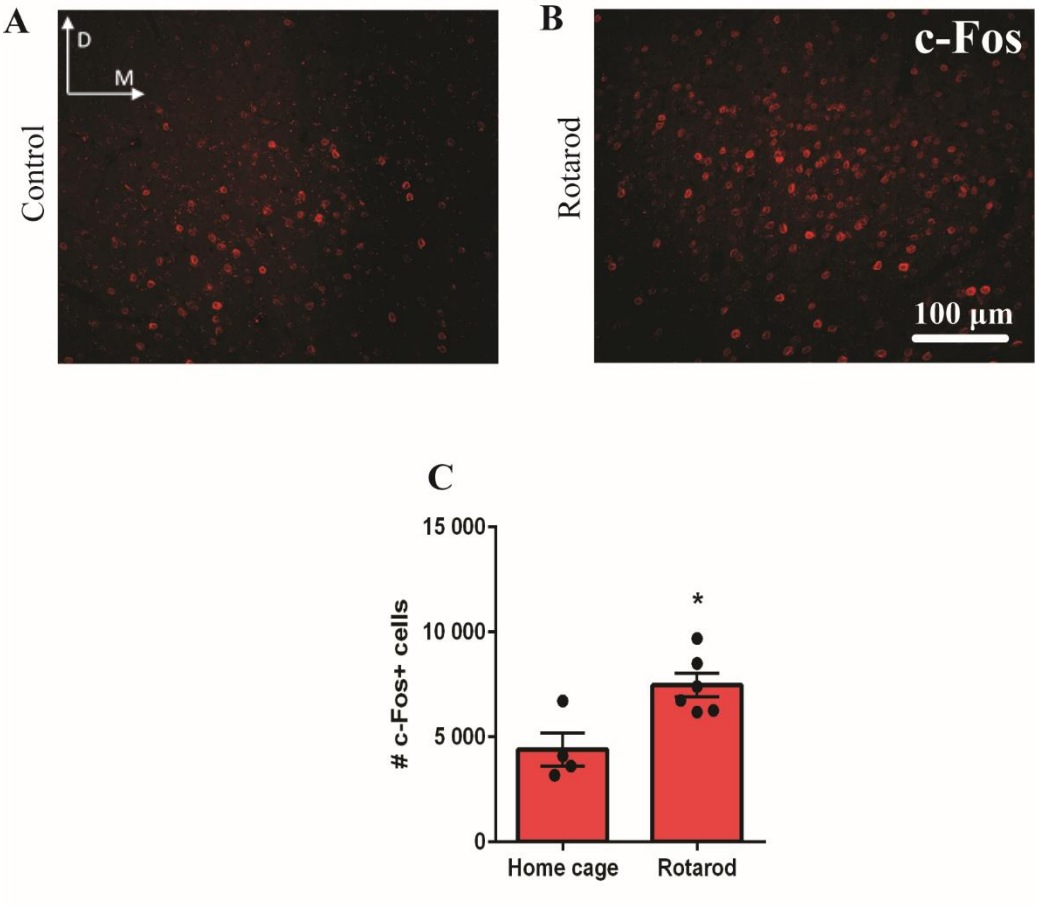

Figure 9: Quantification of c-Fos+ cells labeled during rotarod using OH-Tam dissolved in DMSO and saline (5 mg/kg). Representative images: **A** home cage; **B** rotarod animals. Quantification of c-Fos+ cells (t=3.237, df=8, p=0.0119). Error bars represent SEM.

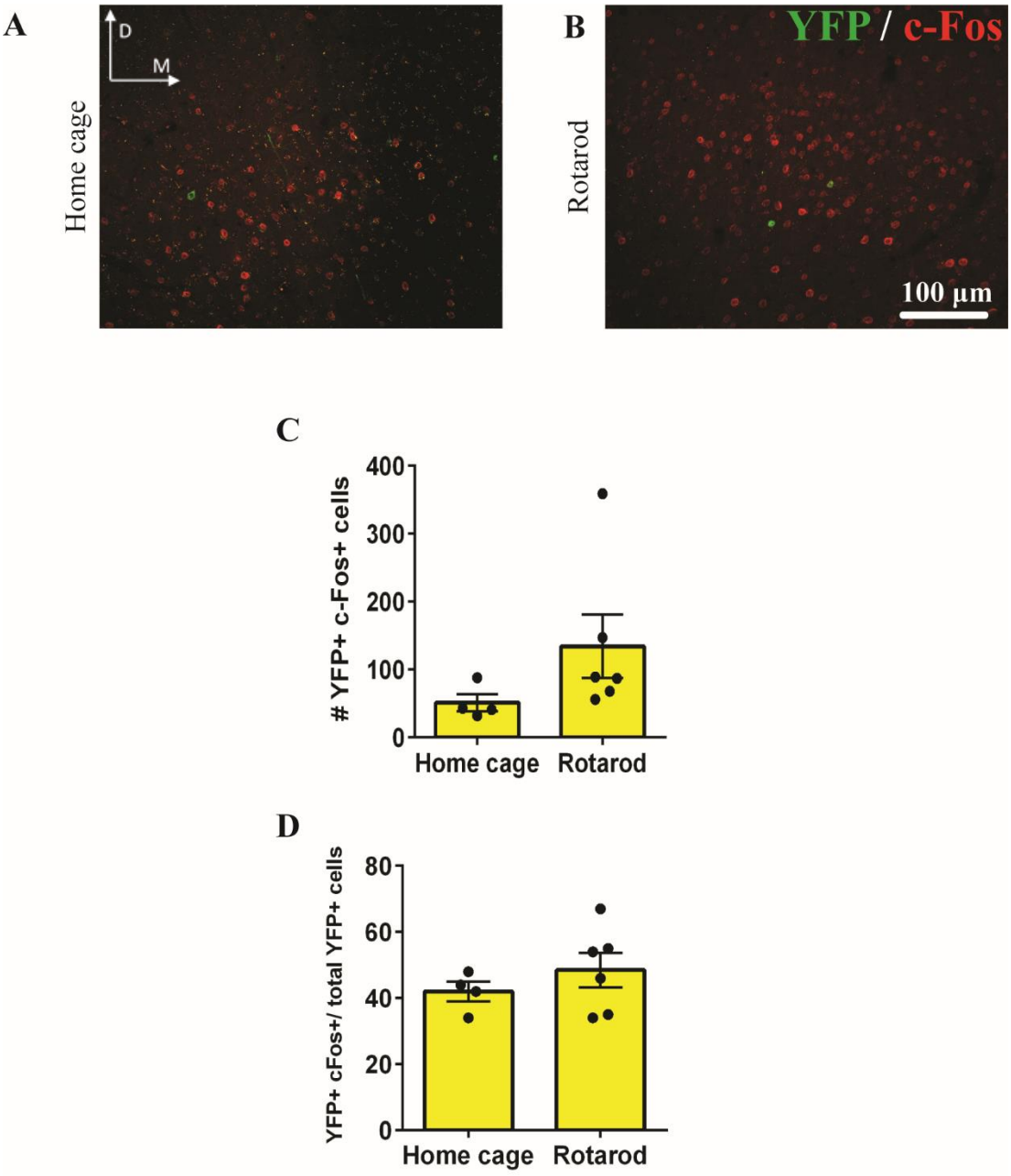

Figure 10: Quantification of c-Fos+ cells labeled during rotarod using OH-Tam dissolved in DMSO and saline (5 mg/kg). Representative images: **A** home cage; **B** rotarod animals. Quantification of c-Fos+ cells (t=3.237, df=8, p=0.0119). Error bars represent SEM.

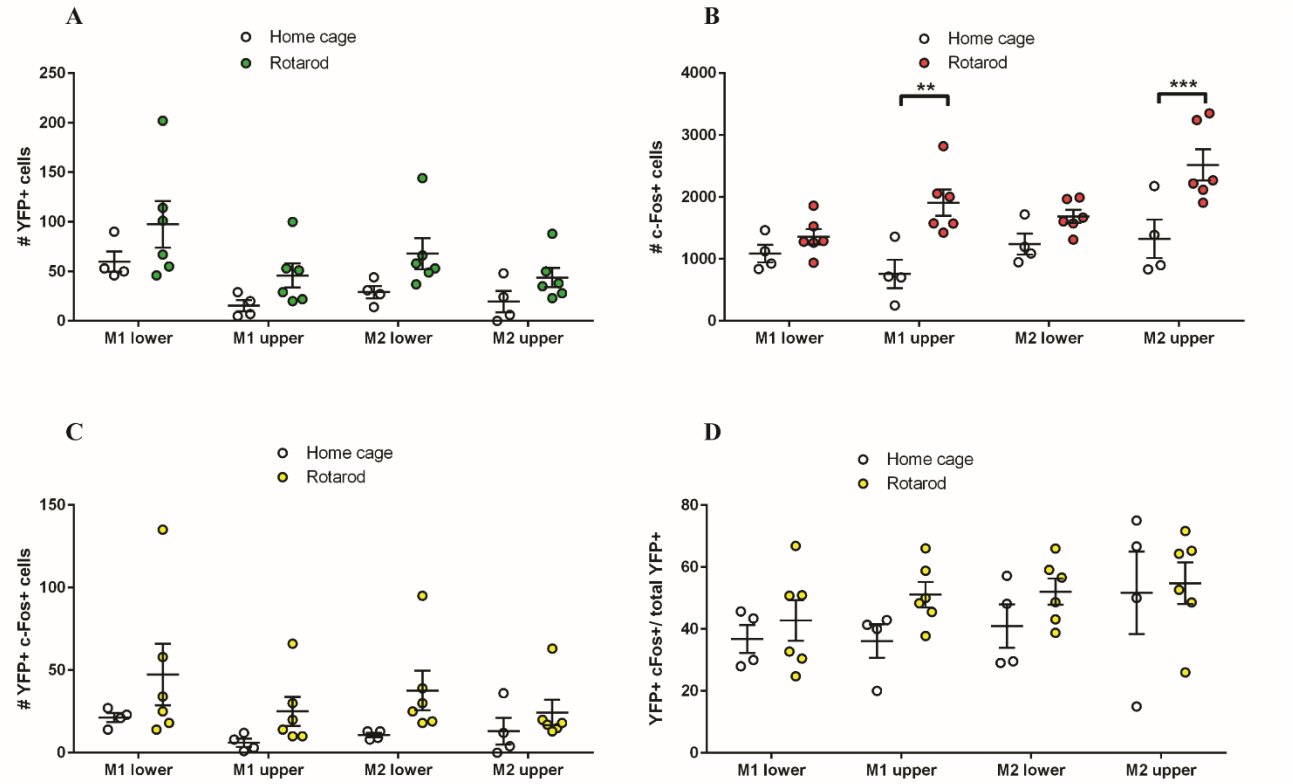

Figure 11: Quantification of colabeled cells during rotarod using OH-Tam dissolved in DMSO and saline (5 mg/kg) by area. **A** Number of YFP+ cells. Significant effect of area ($F_{(3, 24)}$=21.07, p<0.0001), but not of rotarod treatment ($F_{(1, 8)}$=2.824, p=0.1314) or interaction ($F_{(3, 24)}$= 0.4894, p=0.6929). **B** Number of c-Fos+ cells. Significant effects of rotarod treatment ($F_{(1, 8)}$=10.48, p=0.0119), area ($F_{(3, 24)}$=10.41, p=0.0001), and interaction ($F_{(3, 24)}$= 6.257, p=0.0027). After multiple comparisons, significant differences were detected between home cage and rotarod groups in upper M1 (t=3.993, df=32, p=0.0011) and M2 (t=4.142, df=32, p=0.0009), but not lower M1 and M2. **C** Number of YFP+ c-Fos+ cells. Significant effect of area ($F_{(3, 24)}$=5.327, p<0.0059) but not of RR treatment ($F_{(1, 8)}$=1.979, p=0.1971) or interaction ($F_{(3, 24)}$= 0.1.033, p=0.3956). **D** Percentage of YFP+ cells that were also c-Fos+. No significant effect of RR treatment ($F_{(1, 8)}$=1.729, p=0.2249), area ($F_{(3, 24)}$= 2.092, p=0.1279), or interaction ($F_{(3, 24)}$= 0.4565, p=0.7151).

Does increasing the dose of OH-Tam delivered in saline result in more labeling?

To determine whether increasing the dose of OH-Tam would result in more YFP labeling, another cohort of mice was put through the same experimental paradigm, except this cohort received a 40 mg/kg dose of OH-Tam three hours post-behaviour (Figure 12A).

Pre-exposure performance was similar to that of prior experiments and did not show any difference in rotarod performance on the day of OH-Tam or sacrifice (Figure 12B-G). Analysis of labeled cells showed that mice exposed to the rotarod had significantly more YFP+, c-Fos+, and YFP+ c-Fos+ cells than home cage controls (Figure 13C-E). Rotarod mice also had a significantly higher percentage of YFP+ cells that were also c-Fos+ (Figure 13F). When cell counts for this experiment were separated by area (Figure 14), it appeared that all areas showed an increase in the number of YFP+, c-Fos+, and YFP+ c-Fos+ cells. All areas also showed an increase in the percentage of YFP+ cells that were also c-Fos+. The difference in number of YFP+ and colabeled cells between rotarod animals and home cage controls was greatest in the lower M1 and M2 cortices. These results show that this labeling paradigm can label and differentiate between mice performing rotarod and home controls, thus suggesting that this labeling method is activity-dependent.

Are cells active at the OH-Tam the same cells active at the sacrifice time point?

To further shed light on the reliability of this model to examine reactivation of the same motor network at different behavioural time points, another cohort of animals performed rotarod in conjunction with OH-Tam administration, but not at the point of sacrifice (Figure 15A). These animals should therefore have similar levels of YFP labeling to the rotarod animals in the previous experiment (Figure 13C). These mice should also

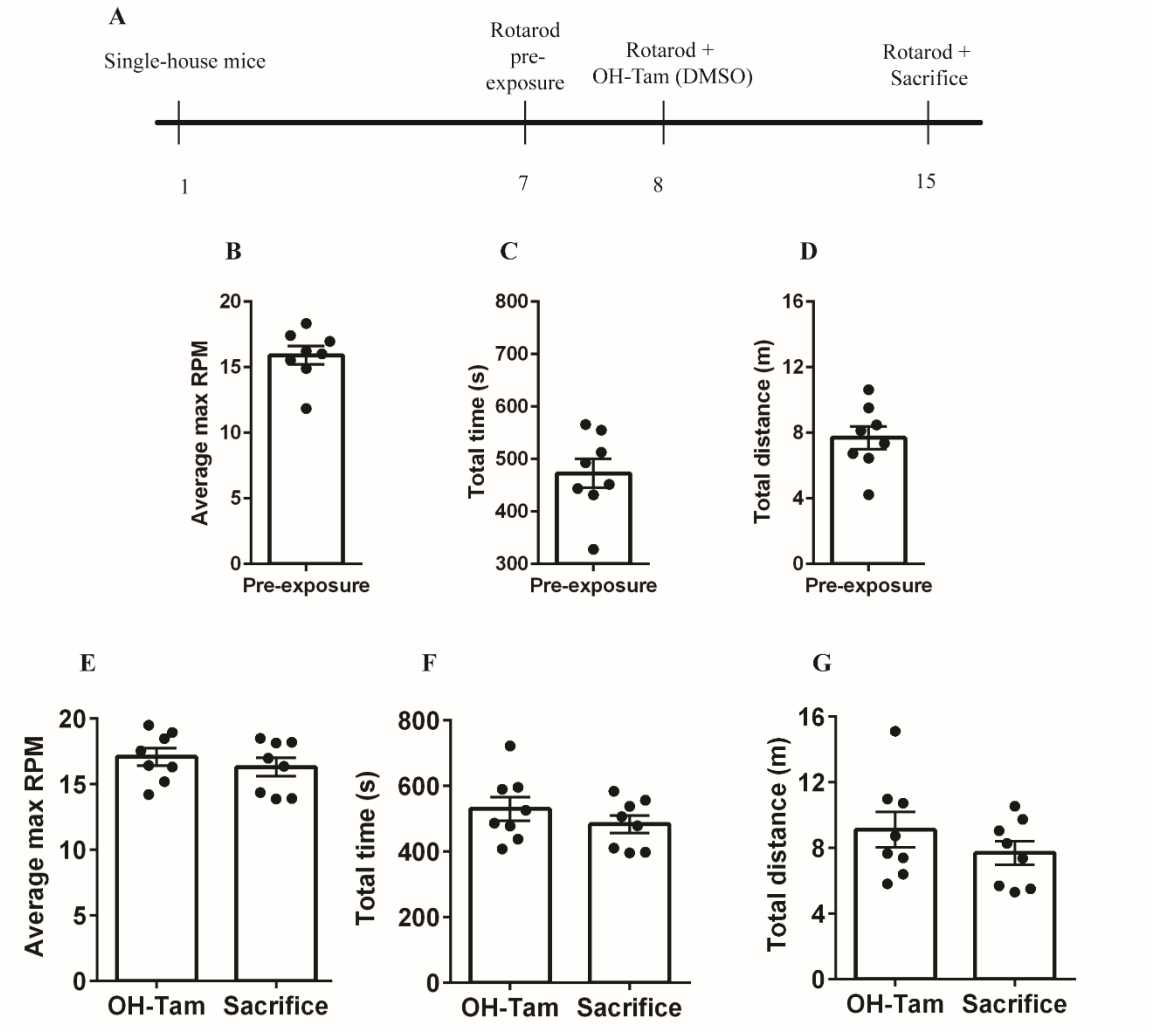

Figure 12: Labeling of networks active during rotarod using OH-Tam dissolved DMSO and saline (40 mg/kg). **A** Timeline of experiment. Rotarod performance during pre-training: **B** average maximum rotation speed; **C** time; **D** distance traveled. Rotarod performance on day of OH-Tam injection and sacrifice: **E** average maximum rotation speed; **F** time; **G** distance traveled. Error bars represent SEM.

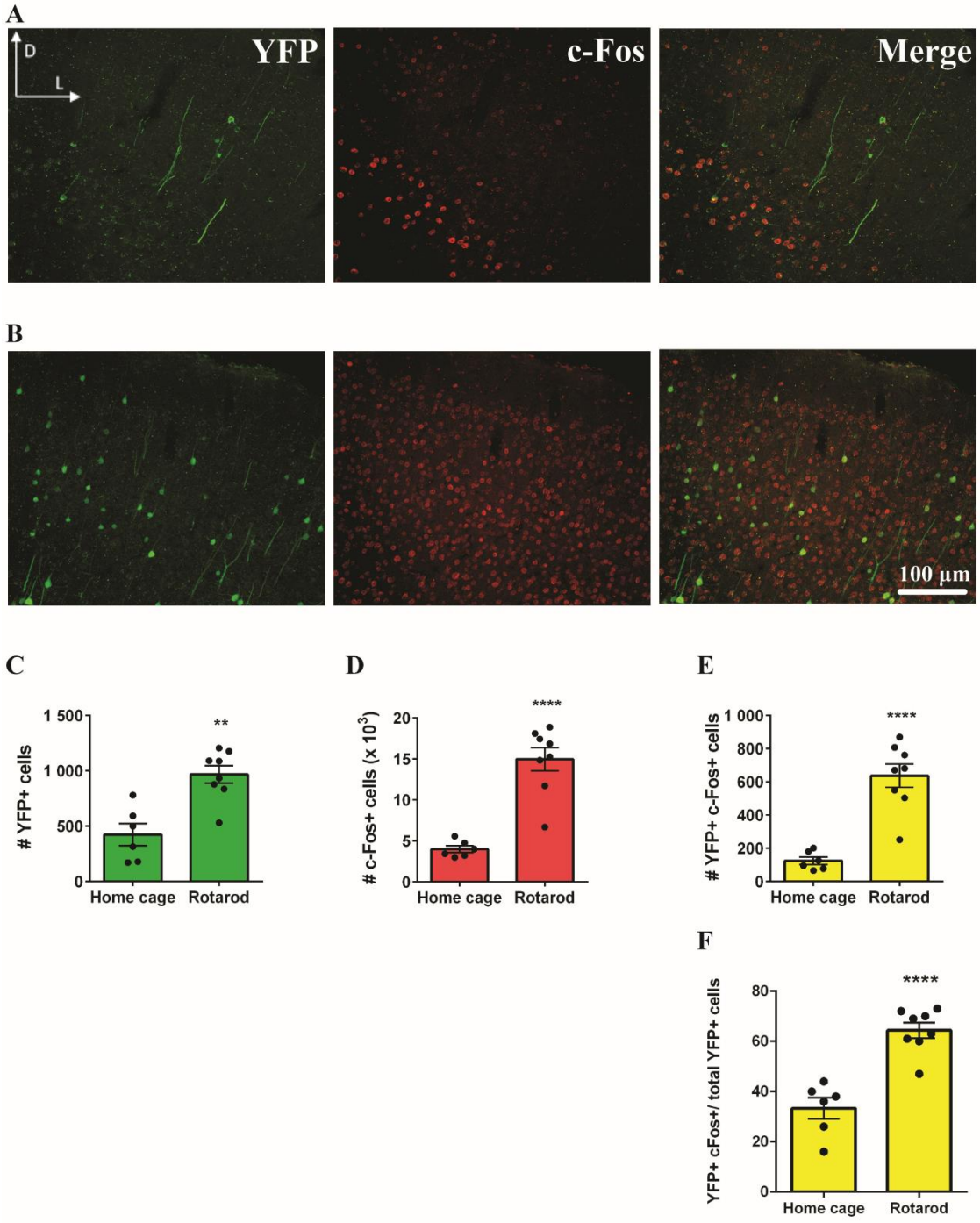

Figure 13: Quantification of cells labeled during rotarod using OH-Tam dissolved in DMSO and saline (40 mg/kg). Sample images of **A** Home cage and **B** Rotarod animals. Quantification of: **C** YFP+ (t=4.340, df=12, p=0.001); **D** c-Fos+ (t=6.454, df=12, p<0.0001) **E** YFP+ c-Fos+ (t=6.087), df=12, p<0.001) cells; **F** percentage of YFP+ that were also c-Fos+ (t=6.112. df=12, p<0.0001). Error bars represent SEM.

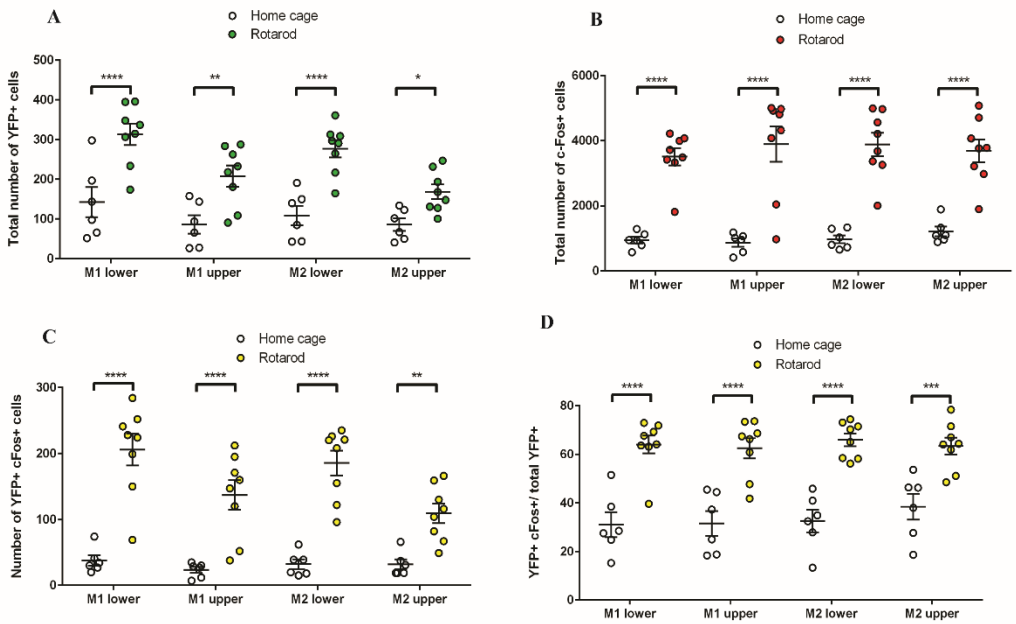

Figure 14: Quantification of colabeled cells during rotarod using OH-Tam dissolved in DMSO and saline (40 mg/kg) by area. **A** Number of YFP+ cells. Significant effect of RR treatment ($F_{(1, 12)}$=18.86, p=0.0010), area ($F_{(3, 36)}$=20.19, p<0.0001), and interaction ($F_{(3, 36)}$=4.361, p=0.0102). After multiple comparisons, significant differences were detected between home cage and rotarod groups in lower M1 (t=4.764, df=48, p<0.0001), upper M1 (t=3.409, df=48, p=0.0027), lower M2 (t=4.698, df=48, p<0.0001), and upper M2 (t=2.300, df=48, p=0.0258). **B** Number of YFP+ cells. No significant effect of area or interaction. Significant effect of RR treatment ($F_{(1, 12)}$=41.65, p<0.0001). After multiple comparisons, significant differences were detected between home cage and rotarod groups in lower M1 (t=5.473, df=48, p<0.0001), upper M1 (t=6.410, df=48, p<0.0001), lower M2 (t=6.166, df=48, p<0.0001), and upper M2 (t=5.253, df=48, p<0.0001). **C** Number of YFP+ c-Fos+ cells. Significant effect of RR treatment ($F_{(1, 12)}$=37.06, p<0.0001), area ($F_{(3, 36)}$=11.12, p<0.0001), and interaction ($F_{(3, 36)}$=8.092, p=0.0003). After multiple comparisons, significant differences were detected between home cage and rotarod groups in lower M1 (t=6.878, df=48, p<0.0001), upper M1 (t=4.643, df=48, p<0.0001), lower M2 (t=6.265, df=48, p<0.0001), and upper M2 (t=3.161, df=48, p=0.0027). **D** Percentage of YFP+ cells that were also c-Fos+. No significant effect of area or interaction. Significant effect of RR treatment ($F_{(1, 12)}$=36.45, p<0.0001). After multiple comparisons, significant differences were detected between home cage and rotarod groups in lower M1 (t=5.529, df=48, p<0.0001), upper M1 (t=5.175, df=48, p<0.0001), lower M2 (t=5.583, df=48, p<0.0001), and upper M2 (t=4.176, df=48, p=0.0001). Error bars represent SEM.

have levels of c-Fos labeling to the home cage controls of the previous experiment (Figure 13D).

Rotarod performance (Figure 15B-G) was similar between this experiment and the last (Figure 12B-G). Analysis of YFP+ cells demonstrated that animals in this experiment had a similar number and distribution of YFP+ cells in the motor cortex when compared to the rotarod animals of the previous experiment (Figure 16B compared to Figure 13C). There was also a similar number of c-Fos+ cells to the home cage controls of the previous experiment (Figure 16E compared to Figure 13D). These animals also had a similar number of colabeled cells, and a similar percentage of YFP+ cells that were also c-Fos+ to the control animals of the previous experiment (Figure 16H and J compared to Figure 13E and F, respectively). This result also suggests that this model, when used in conjunction with 40 mg/kg OH-Tam delivered in saline, reliably labels networks in the motor cortices recruited by a motor task.

Is our c-Fos staining protocol sensitive enough to detect differences in rotarod behaviour?

To determine whether our c-Fos staining protocol was sensitive enough to detect differences in c-Fos expression between animals that traveled different distances on the rotarod, all rotarod and c-Fos data was pooled from the experiments in which in animals performed RR at endpoint (Figure 17; pooled animals described in Figures 6A and 12A). We hypothesized that there would be a positive correlation between rotarod performance and the number of c-Fos+ cells. Indeed, there was a significant positive correlation between the number of c-Fos+ cells and rotarod performance. This suggests that the c-Fos staining protocol used is sufficiently sensitive to detect differences in the number cells active during RR performance.

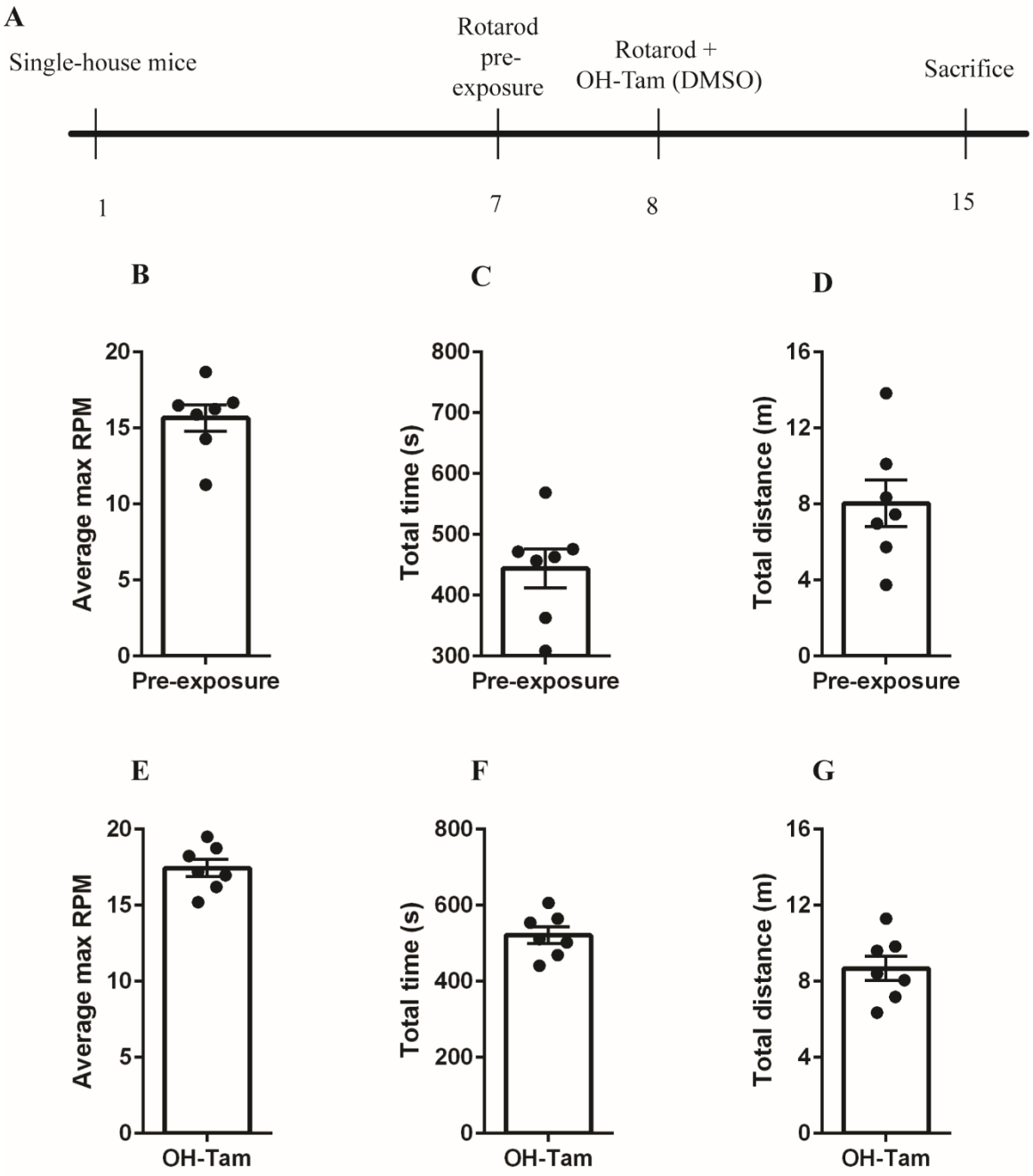

Figure 15: Labeling of networks active during one rotarod exposure. **A** Timeline of experiment. Rotarod performance during pre-training: **B** average maximum rotation speed; **C** time; **D** distance traveled. Rotarod performance on day of OH-Tam injection and sacrifice: **E** average maximum rotation speed; **F** time; **G** distance traveled. Error bars represent SEM.

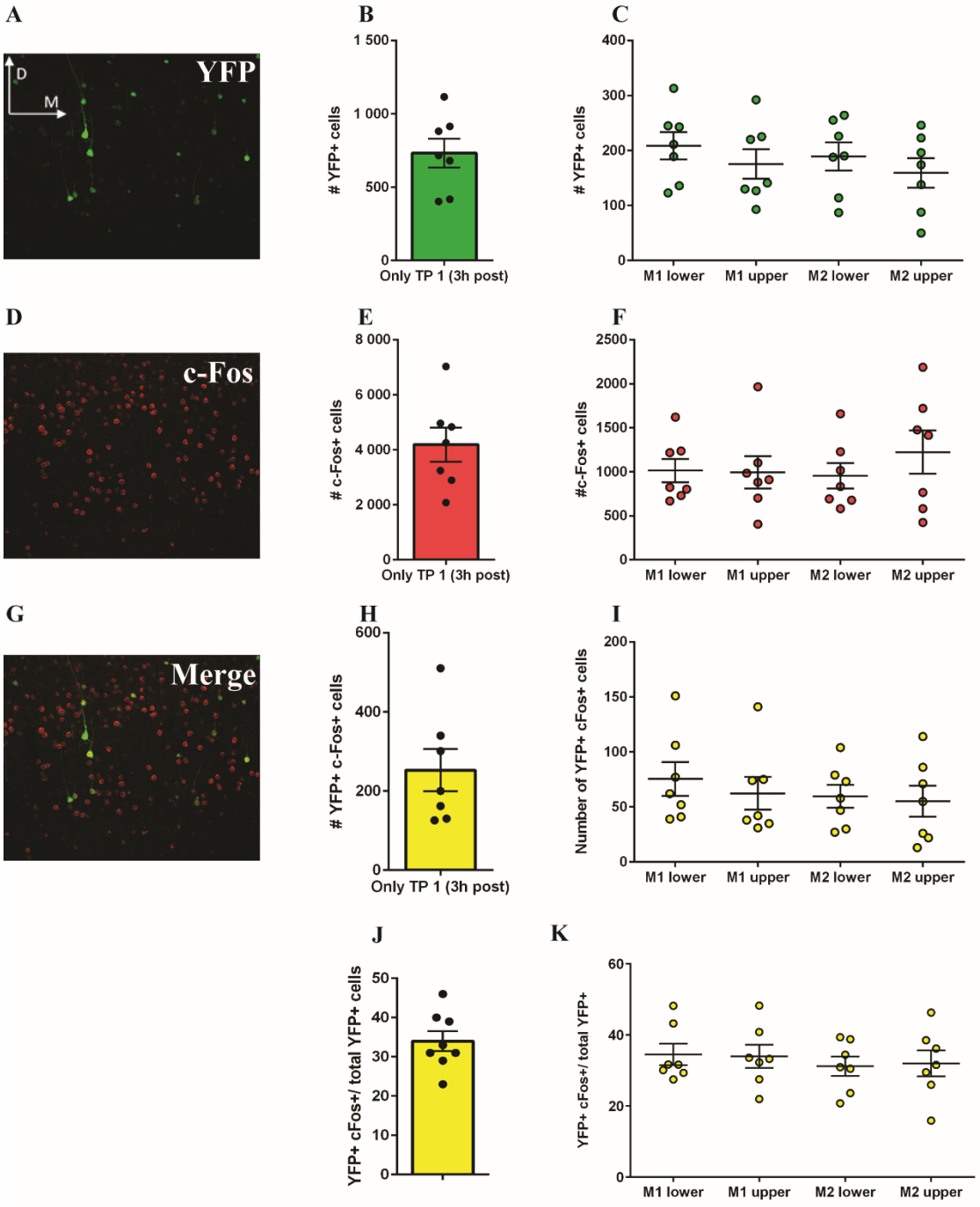

Figure 16: Quantification of cells active during rotarod at time of OH-Tam injection, and in home cage at time of sacrifice. Representative images, counts of total number of cells, and counts of cells separated by area for: **A-C** YFP+; **D-F** c-Fos+; **G-I** YFP+ c-Fos+ cells. **J** Percentage of YFP+ cells that were also c-Fos+. **K** percentage of YFP+ cells that were also c-Fos+ separated by area.

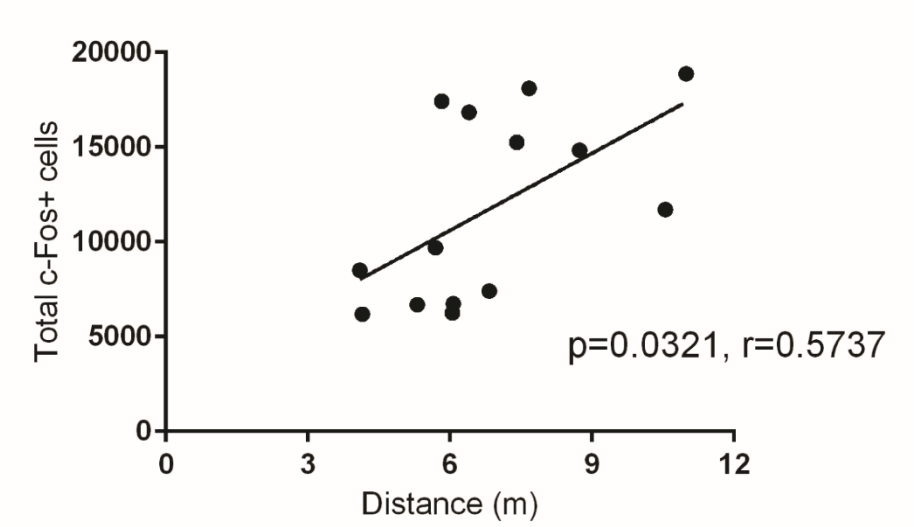

Figure 17: Correlation of total number of c-Fos+ cells with distance traveled on the rotarod (n=14).

Aim 2: Pilot study to determine if stimulation of the contralesional motor cortex alters functional recovery.

To determine whether contralesional activation of neurons can influence stroke recovery, we made use of the same Arc-CreER^{T2} mouse, this time crossed with a floxed-STOP-ChR2 mouse to make Arc-ChR2 mice. The resulting mouse model allowed us to express ChR2 in cells that were recruited by a behavioural task.

As described in Figure 18A, after being implanted with a fiber optic wire in the right M1, mice were individually-housed. Two weeks later, all mice began pre-training on the adhesive removal test, and were tested for baseline cylinder performance. Mice which displayed a unilateral deficit on either task or did not learn the adhesive removal task were excluded (six and three mice, respectively). After pre-training on the adhesive and cylinder tasks, mice were given a PT stroke in their right M1. These experiments were performed using the OH-TAM protocol developed by Denny et al. (2014[63]) and prior to our studies above using Ye et al. (2016[67]) .

The day after stroke, mice were placed into a dark room. On the second day after stroke, mice were given an injection of OH-Tam in oil and ethanol, followed by the adhesive removal task five hours later. Mice were left in the dark for two days after OH-Tam injection to mitigate the risk of non-task-related recombination. To confirm stroke-induced behavioural deficits, post-stroke behaviour testing was completed during the first week after stroke. The adhesive test was repeated on the third day post-stroke, and the cylinder test was performed on the fourth day after stroke. After the first round of post-stroke behavioural testing, mice were assigned one of either the control or the group that received optogenetic stimulation (stim) groups. The control group underwent the same procedures as the stim group but did not receive optogenetic stimulation. Six days after

stroke, mice began receiving daily optogenetic stimulation (Figure 18B-D) of the contralesional M1 in the home cage. On the day of endpoint, mice received optogenetic stimulation and were sacrificed 90 minutes later.

After five days of training on the adhesive task, mice learned to contact and remove the pieces of tape (Figure 19A-B). On average, at two-three days post-stroke both the time to contact and time to remove the tape from the paw contralateral to the stroke was longer than during pre-stroke performance. Although the average times for both time to contact and remove were longer post-stroke, this was only significant for the control mice. We believe this is due to the large amount of variability in the data as well as the relatively small sample size of this pilot experiment.

The same analysis of the group that later received optogenetic stimulation revealed non-significant deficits on the time to remove the tape. Three weeks after stroke, although it seemed that neither group's performance returned entirely to baseline, it appeared that the control group recovered slightly more than the group that received stimulation. However, the large amount of variability observed prevented definite conclusions from being drawn.

Before stroke, both the control and stim groups used their paws equally when rearing in the cylinder. After stroke, both groups used their contralesional paw significantly less. While there was a significant increase in the control group's affected paw use three weeks after stroke, there was no such increase in the stim group. Taken together, these preliminary data obtained with a relatively small sample size suggest that the stimulation of the contralesional network recruited two days post-stroke hinders recovery.

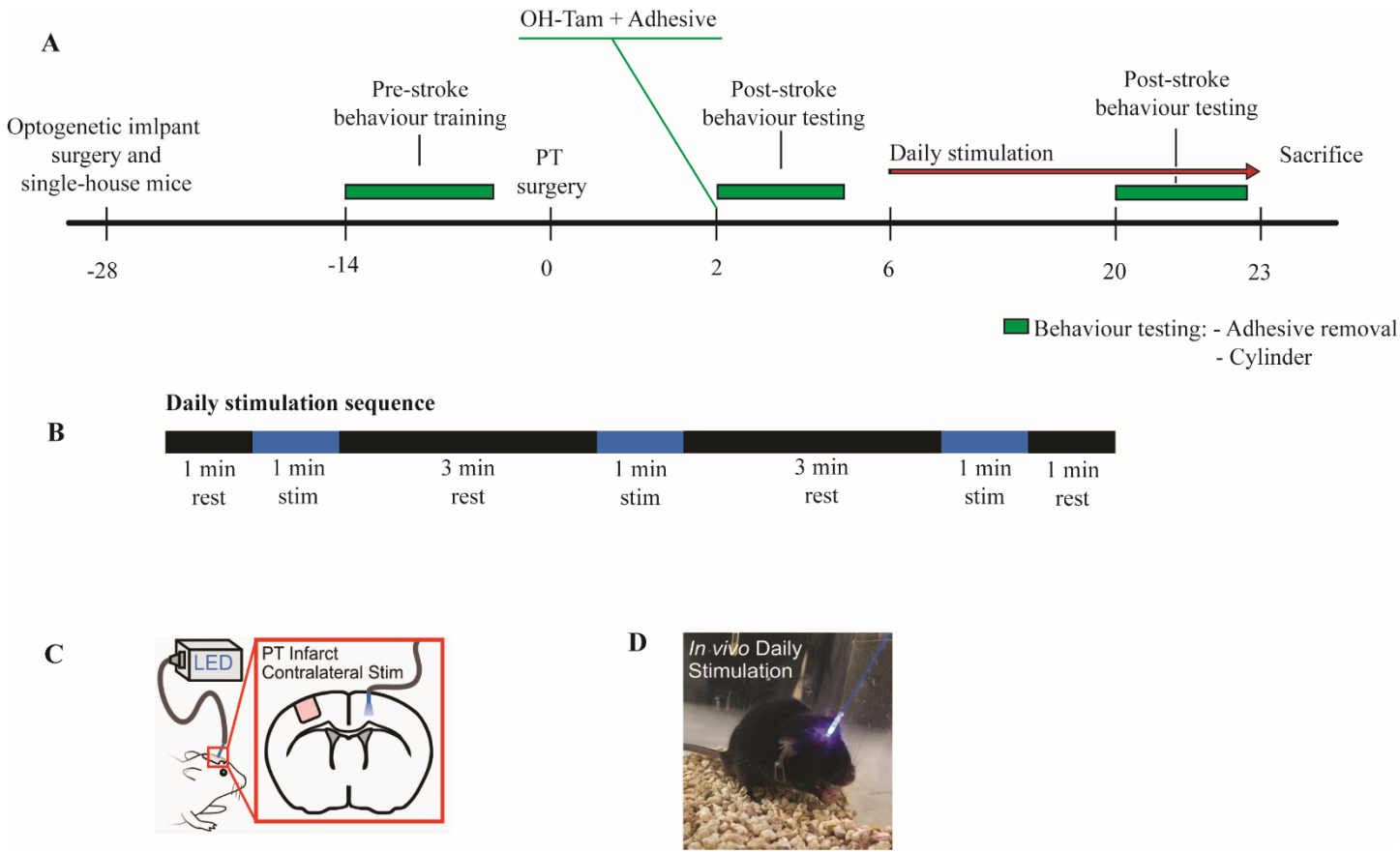

Figure 18*:* In vivo optogenetic stimulation of the contralesional cortex. **A** Experimental timeline. **B** Sequence of daily optogenetic stimulation. **C** Schematic of stimulation and stroke location. **D** Picture of mouse receiving stimulation.

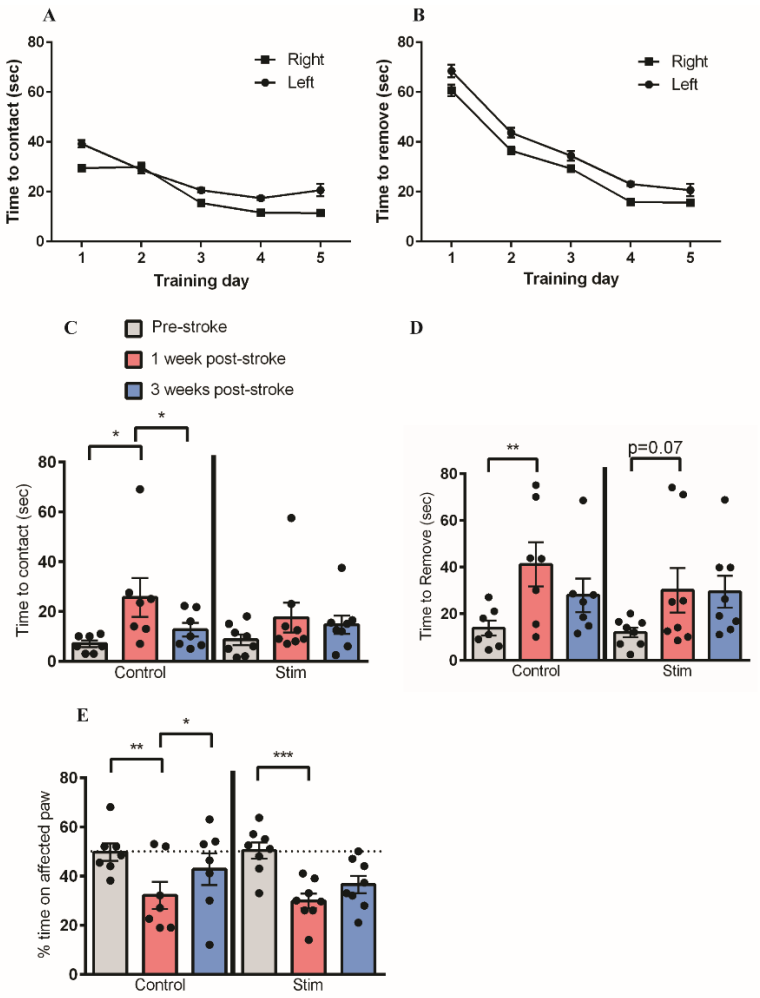

Figure 19: Daily optogenetic stimulation of the contralesional cortex prevents SBR. **A** Adhesive contact training. **B** Adhesive removal training. **C** Adhesive contact performance before stroke, one week post-stroke, and three weeks post-stroke. Significant effect of time ($F_{(2, 26)}$=5.126, p=0.0133), but not of stimulation treatment or interaction. Sham-stimulated animals displayed a difference in performance when comparing pre-stroke to one-week post-stroke (t=2.956, df=26, p=0.0131) and one- to three-week post-stroke performance (t=2.058, df=26, p=0.0498). **D** Adhesive removal performance before stroke, one week post-stroke, and three weeks post-stroke. Significant effect of time ($F_{(2, 26)}$=7.311, p=0.0030), but not of stimulation treatment or interaction. Sham-stimulated animals displayed a difference in performance when comparing pre-stroke to one-week post-stroke performance (t=3.069, df=26, p=0.0099). Stimulated animals showed a trend toward significance when comparing pre-stroke to one week post-stroke performance (t=2.184, df=26, p=0.0763). **E** Cylinder performance before stroke, one week post-stroke, and three weeks post-stroke. Significant effect of time ($F_{(2, 26)}$=18.18, p<0.0001), but not of stimulation treatment or interaction. Significant differences in pre-stroke versus one week post-stroke performance were detected in both the sham-stimulated (t=3.806, df=26, p=0.0015) and stimulated groups (t=4.747, df=26, p=0.0001). Significant differences in one week versus three week post-stroke performance was detected in the group that received sham stimulation (t=1.545, df=26, p=0.0294).

Stroke volumes

To verify whether the effects of optogenetic stimulation on adhesive and cylinder performance were due to differences in the size of the strokes, lesion volume analysis was performed. There was no significant difference in lesion volume between animals that received optogenetic stimulation and sham stimulation (Figure 20). This supports our hypothesis that the optogenetic stimulation of the contralesional hemisphere does not affect stroke size and lends strength to our conclusion that contralesional stimulation has a deleterious effect on stroke recovery.

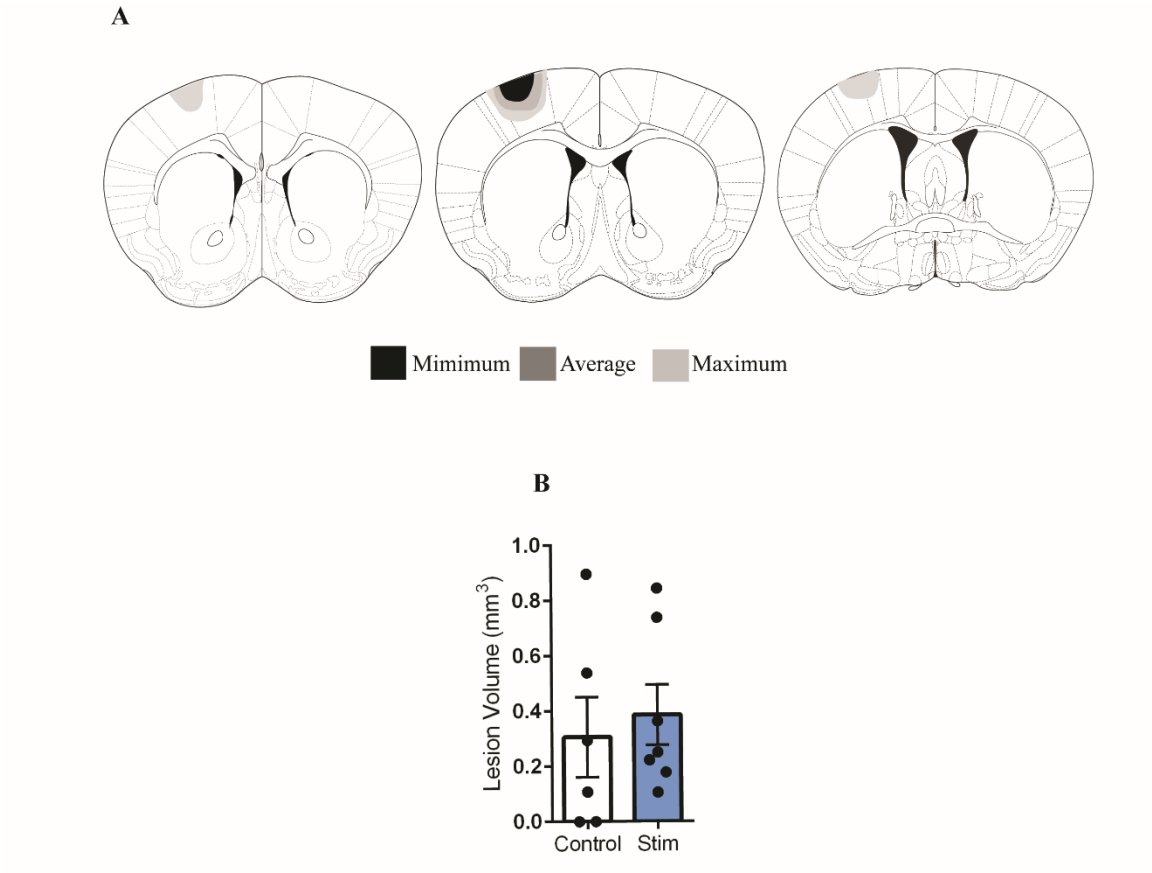

Figure 20: Daily optogenetic stimulation of the contralesional cortex does not alter lesion volume. **A** Representative schematic. **B** Stroke volume (t=0.4512, df=11, p=0.6606).

5. Discussion

Elucidating the biology underlying the plasticity observed following a stroke, including the reorganization of motor control, should facilitate the discovery of new treatments which harness this plasticity for therapeutic gains. In humans and animal models, the functions governed by the stroke-afflicted region can be reallocated to many different brain regions. However, the specific types of cells being recruited in these regions remain elusive. The experiments in Chapter 1 of this thesis demonstrate the feasibility and validity of using a TRAP mouse model to label cells active during a behavioural task. Specifically, we demonstrate the ability of the ArcCreER^{T2} model to label cells recruited during the rotarod task, as supported by a significant correlation between number of cells labeled and performance on the rotarod task. Further, we show that 65% of these cells within the motor cortex are reactivated when performing this task a second time. In Chapter 2, experiments combine the use of the Arc-ChR2 mouse with optogenetics to evaluate the effect of daily stimulation of the contralesional motor cortex cells used to perform the adhesive removal task in the acute phase of stroke recovery. The findings from this pilot study demonstrate the feasibility of this approach and suggest stimulation of these contralesional cells may reduce recovery. Together, the results from both of these chapters set the groundwork for the use of this model to investigate the cells used to perform a motor task before stroke, and during the various stages of recovery.

Aim 1: Evaluating the ability of the ArcCreER^{T2} mouse to label cells recruited to perform a motor task

When using the adhesive test to label the active network, our results showed that the labeling in the motor cortex was dependent on OH-TAM treatment but was unexpectedly not dependent on performance of the adhesive task. There were no

differences observed in the number of active YFP+ cells in the motor cortex between home cage control animals and those performing the adhesive task. We hypothesized that this lack of difference could be due to the animals being able to remove the tape very quickly, with an average of 15 seconds (range 10-30 seconds). Since OH-TAM has been shown to be bioavailable for four to six hours when administered in oil and EtOH[60,67], this suggests that this paradigm is not sensitive enough to use with the adhesive task. Thus, since the task was so short compared to the labeling window, it may not have induced enough of an increase in activity from the baseline level induced by home cage activities, such as grooming, eating, and nest-building. In support of this hypothesis, all other publications using TRAP models have made use of stimuli that were salient and/or repetitive stimuli[60,63,64,66,67]. These include foot shocks, cocaine, flashing lights, and exposure to odours, all of which are likely to elicit more activity in their respective brains than a single 15-second bout of tape removal in the motor cortex. These results therefore suggest a limitation of TRAP models may be that they cannot reliably label cells activated during the adhesive task.

Since the rotarod task had been shown to induce strong activation of the motor cortices in Arc-GFP reporter mice[58,70], this task was utilized to test the ability of a variety of OH-TAM treatment paradigms to detect activity-dependent labeling within the motor cortex. When using the same OH-Tam administration paradigm as Denny et al. (2014[63]), administered in oil and EtOH with the rotarod behavioural task, surprisingly there was not a difference in the number of labeled cells between animals that remained in their home cage and those performing the rotarod task. In comparison to other TRAP studies[63] our results showed more labeled cells in the motor cortex of the home cage control mice. This

paradigm did work previously in the hippocampus[63,66], which could perhaps be due to the lower level of background activity in this area, as well as the salient nature of foot shocks used in their fear conditioning task. Together, these factors likely resulted in a better signal-to-noise ratio, and thus more specific labeling.

Through another series of experiments that utilized a different method of administering OH-Tam in saline and DMSO[67,74], and modifying the dosage of OH-TAM, we established a protocol that showed the Arc-CreER^{T2} mice could be used reliably to label activity-dependent behavior. This protocol used the same OH-Tam administration paradigm as published by Ye et al. in 2016, which has a one- to two-hour labeling window[67], except that the dosage of OH-Tam was increased to 40 mg/kg. In support of this treatment working, the rotarod animals had significantly more YFP+ cells and c-Fos cells, when compared to the home cage control animals. Additionally, another experiment in which mice performed rotarod at the time of OH-Tam injection but not at the time of sacrifice showed the ability of this model to specifically label cells recruited by a behavioural task. These animals had a similar number of YFP cells to mice that performed the rotarod task in other experiments using the same OH-Tam treatment paradigm, and as expected, also had a similar number of c-Fos cells to the control group. Thus, this treatment paradigm appeared to allow for the labeling of cells active during rotarod performance. However, it remains to be determined if increasing the dose of OH-Tam for this treatment paradigm alters the window; it is possible that an increase in OH-Tam dose lengthens the labeling window. Future experiments will therefore evaluate how adjusting the time between OH-Tam administration and rotarod behaviour alters the number of YFP+ cells labeled.

One of the greatest advantages of TRAP models is their ability to label neurons active at two behavioural time points. In other publications, cells active at a first behavioural time point were labeled using indelible fluorophores such as YFP[63] or tdTomato[65,67]; whereas cells active at the second time point are labeled using IHC for various IEGs, such as Arc or c-Fos[63,67]. The decision to use c-Fos as a marker of activity at the second behavioural time point was made for two reasons. Most importantly, it is a better choice as a marker of activity than Arc since Arc mRNA has recently been shown to be shuttled between cells[75,76]. This could potentially lead to the translation of Arc protein in neighboring cells which are not active. Second, since Arc protein is highly enriched in the dendrites, and since YFP is most concentrated in the soma, collocating the two is more difficult than collocating YFP with a nuclear antigen such as c-Fos. It had been previously determined that Arc and c-Fos have similar activation kinetics[55]. Therefore, it was not surprising that they colabeled at 96% when the animals were made to perform the rotarod task and sacrificed 90 minutes later. Given the advantages of using c-Fos and its similarity in activation kinetics to Arc, c-Fos was the best choice of IEG to use in this project.

After separating our analysis of active cells by region in both motor cortices, it was clear that the increase in number of cells in the rotarod group came from an increase in the upper layers of M1 and M2. The flow of information in the motor cortex generally runs from the superficial to the deep layers, with the former mostly receiving input from the sensory cortices and the latter from the frontal cortices[77,78]. Thus it is possible that this increase in activity in the upper layers of the motor cortex is originating in the sensory cortices. These results are not completely in accordance with the results obtained by Cao et al.[70], in which they found that there was a larger increase in cells specifically in M2 over

M1 from a similar rotarod paradigm using an Arc-GFP reporter mouse. Our results suggest an equal activation of M1 and M2, specifically the upper areas of these regions. One potential difference in our findings could be attributed to differences in analysis, with our work counting total cells and Cao et al.[70] examining cell counts per unit area. Thus future work could reanalyze our results using stereological assessments. In order to paint a more complete picture of the activation occurring during rotarod, the phenotype of the active neurons would also need to be determined. This can be accomplished by staining for markers of excitatory and inhibitory neurons, such as the vesicular glutamate transporter (VGLUT) or the vesicular GABA (gamma-aminobutyric acid) transporter.

Another interesting finding from these studies using the different treatment paradigms has been that the number of c-Fos+ or Arc+ cells has consistently been much greater than the number of YFP+ cells. This result has been obtained by others using TRAP models[67], although never well-discussed. It could be due to a difference in the ability of these mice to label active cells at the first time point with YFP, versus the endogenous expression of c-Fos or Arc which are detected by IHC at the second time point. In relation to this, there are notable differences in the level of brightness in the c-Fos+ or Arc+ IHC-labeled cells, as has also been observed by others[54]. This raises the question of whether all c-Fos+ cells were active to the same degree. It is possible that staining with a more dilute concentration of the c-Fos antibody would result in the detection of only the brightest cells observed using this current protocol (data not shown). In the future, it may be interesting to analyze the degree of colocalization of c-Fos and YFP in cells of varying c-Fos immunofluorescence intensity. Our analysis, however, was using c-Fos antibody at a level that detected all c-fos expressing cells (determined through a dilution curve, not shown)

and appeared to be specific. This is also further supported by the significant positive correlation between the number of c-fos+ cells and distance mice traveled on the rotarod.

There are additional experiments that would help determine the sensitivity and reliability of the Arc-CreER^{T2} model to measure cells active during motor tasks. For example, unilateral and bilateral stimulation of the forepaw of the animals would allow us to assess the degree to which stimulation elicits activation in the brain, as was done by Guenthner et al. (2013[65]). This would have the advantage of avoiding usage or activation of the paws through home cage behaviours such as walking or grooming. Additionally, it will be helpful to assess the ability of this model to label cells active during a unilateral behaviour task. The expected outcome of this work based on the work of others showing regional reorganization[65], would be a robust increase in the number of YFP+ cells labeled on the side contralateral to the paw being used to do behaviour, in comparison to minimal activation in the ipsilateral cortex. This work is especially important for our future aims in stroke recovery, since stroke induces unilateral deficits, and contralateral activation has been observed following stroke[56,79]. Given our findings in this study that show that this model can be used to identify active cells, it is exciting to think of the potential of this model to examine 1) the cells active before stroke and in the acute phase of stroke recovery, and 2) the cells active during the acute and chronic phases of SBR. Additionally, combining this model with the use of whole-brain imaging, as was done in the paper by Ye et al. (2016[67]) would provide information on how cells are reorganizing in the brain.

Aim 2: Optogenetic activation of the contralesional motor cortex impairs SBR

In this pilot experiment, we sought to determine the effect of daily stimulation of cells active in the contralesional motor cortex during a behavioral task with the goal of

determining if this would alter functional recovery. This was the first set of experiments in our lab combining the use of the Arc-CreER^{T2} model and *in vivo* stimulation. These studies were performed in concert with the work described in Chapter 1. Many experiments not included in this thesis sought to establish the methodology required for the completion of this pilot experiment. These included, for example, experiments to establish the optogenetic stimulation apparatus.

From the small sample size of this pilot experiment, it appeared that the mice that received stimulation had a reduction in recovery. This effect was most pronounced in the results obtained from the cylinder task. The results obtained from the adhesive removal task were trending towards significance, and confounded by differences in baseline deficits between the control group and the group that received optogenetic stimulation. Overall these results demonstrate the feasibility of the methodology to perform this study and encourage future studies to use this model.

There were limitations of this pilot experiment presented in Chapter 2 which prevented us from drawing any definitive conclusions and would need to be adjusted prior to performing future experiments. First, the paradigm used to label cells recruited by the adhesive removal task post-stroke was also not optimal since these studies were performed prior to the work shown in Chapter 1. By administering OH-Tam in oil and EtOH, it is conceivable that we were labeling and therefore stimulating cells that were not related to performing the adhesive task. This would make our results less like those of previous TRAP papers[63,64], and more like those which used transgenic models to stimulate all neurons in a specific area[49,50]. Repeating this experiment using the optimal OH-Tam paradigm described in Chapter 1 should therefore shed light on whether these results

extrapolate to only the active network being labeled. Future work will also confirm which population of cells expressed ChR2 and were being stimulated. This could be performed by using IHC to detect c-Fos+ cells that are also YFP+, as has been done for other previous TRAP papers[63,64].

Despite these limitations, it is interesting to consider how our results compare with the only other preclinical study by Cheng et al. (2014[49]) that has utilized optogenetics to evaluate the effect of stimulation of the contralesional cortex on functional recovery. In this study, no effect of contralesional stimulation was observed. The reason we obtained conflicting results remains unknown, but could be due to differences in stroke size, or number of neurons stimulated. Finally, cells involved in the behavioural task are labeled regardless of phenotype, meaning that TRAP models label cells regardless of their function, be it excitatory, inhibitory, or neuromodulatory. This means that although we are delivering optogenetic stimulation, we might not be exciting to the same degree as if we used a Thy-1-ChR2 mouse.

Indeed, the role of the contralesional cells during stroke recovery has been a rich area of debate[53,80]. After stroke, the contralesional hemisphere is thought to exert an increase in transcallosal inhibition on the ipsilesional cortex. Thus, many have sought to inhibit the contralateral hemisphere, with the hope of reducing this deleterious transcallosal inhibition of the infarcted cortex[81]. This approach is supported by studies proposing that the reestablishment of activity in ipsilesional M1 is perhaps one of the most important factors dictating motor recovery[82], and the degree of transcallosal inhibition from the contra- to the ipsilesional hemisphere is proportional to motor impairment[83]. Thus, our

results support the current literature from human clinical trials that support that contralesional activation is deleterious for recovery[80,81].

Although it cannot be determined from this study, it is interesting to speculate the mechanism by which activation of the contralateral side is deleterious. One hypothesis is that contralesional activation is inhibiting the ipsilesional cortex transcallosally. If this is the cause of the lack of recovery in the group that received optogenetic stimulation, it would follow that ipsilesional stimulation in the same timeframe would ameliorate recovery. Another reason there may not have been recovery in animals that received optogenetic stimulation could be that stimulation reinforces the initial network recruited to perform the behavioural task, and this network is not the same one used at later time points. Hypothetically, normal recovery could entail using different motor networks at two days post-stroke versus at three weeks post-stroke to complete the same task. It would therefore follow that stimulating the network used at two days post-stroke might not allow for normal reorganization or SBR to occur. If this hypothesis is correct, it might be that stimulation of the ipsilesional cortex within this same timeframe is deleterious for recovery as well.

One of the limitations of TRAP models using optogenetics is that labelling and stimulation is behaviour-dependent. As shown in the data presented in this thesis, not all animals had a substantial deficit on the adhesive removal test post, which was used to induce ChR2 expression. Thus in animals without deficits, we might have been stimulating neurons which were normally recruited to perform that behaviour task, whereas in others with deficits, we would have been stimulating the "reorganized" network. Future studies will need to account for this variability when required sample sizes are determined. This limitation, however, can also be a strength. With a large enough sample size, a sub-analysis

of mice with varying degrees of behavioural deficits can be completed. We could therefore investigate whether the results we are observing are the general result of stimulation, or if the effects are dependent on the cell populations initially labeled. Another interesting and important caveat is that all neurons, regardless of their individual level of activity, are labeled if they are active above a certain threshold when OH-Tam is present. Whether it was very active or just active enough to induce ChR2 expression, all labeled cells will express ChR2 to the same degree. Thus, no inferences about the importance of each cell or the role that each cell is playing in the network can be made. More importantly, all cells, regardless of degree of initial activation, will receive the same amount of optogenetic stimulation. This means that some cells which are only meant to be active to a small degree and maybe peripherally related to the motor network will receive the same stimulation as an adjacent cell that is perhaps centrally important to the same network.

6. Conclusion

In this project, we established that the Arc-CreER^{T2} mouse line can be used to determine which cells were recruited during a behavioural task. By testing and modifying two published OH-Tam administration paradigms, we determined the optimal way to dissolve and administer OH-Tam for labeling in the motor cortex. We further found in a pilot study that activation of the contralesional motor cortex may impair functional recovery. This thesis therefore lays some of the essential foundation to evaluate how motor networks reorganize during the various phases of stroke recovery.

7. References

1 Canada, H. S. F. o. Stroke Report. (2017).

2 Andersen, K. K., Olsen, T. S., Dehlendorff, C. & Kammersgaard, L. P. Hemorrhagic and ischemic strokes compared: stroke severity, mortality, and risk factors. *Stroke* **40**, 2068-2072, doi:10.1161/STROKEAHA.108.540112 (2009).

3 Sims, N. R. & Muyderman, H. Mitochondria, oxidative metabolism and cell death in stroke. *Biochim Biophys Acta* **1802**, 80-91, doi:10.1016/j.bbadis.2009.09.003 (2010).

4 Mittmann, N. *et al.* Impact of disability status on ischemic stroke costs in Canada in the first year. *Can J Neurol Sci* **39**, 793-800 (2012).

5 MP, L. *et al. Canadian Stroke Best Practice Recommendations Overview and Methodology*, 2014).

6 Cheng, N. T. & Kim, A. S. Intravenous Thrombolysis for Acute Ischemic Stroke Within 3 Hours Versus Between 3 and 4.5 Hours of Symptom Onset. *Neurohospitalist* **5**, 101-109, doi:10.1177/1941874415583116 (2015).

7 Vivien, D. Can the benefits of rtPA treatment for stroke be improved? *Rev Neurol (Paris)*, doi:10.1016/j.neurol.2017.07.003 (2017).

8 Goyal, M. *et al.* Randomized assessment of rapid endovascular treatment of ischemic stroke. *N Engl J Med* **372**, 1019-1030, doi:10.1056/NEJMoa1414905 (2015).

9 Saver, J. L. *et al.* Time to Treatment With Endovascular Thrombectomy and Outcomes From Ischemic Stroke: A Meta-analysis. *JAMA* **316**, 1279-1288, doi:10.1001/jama.2016.13647 (2016).

10 Vidale, S. & Agostoni, E. Endovascular Treatment of Ischemic Stroke: An Updated Meta-Analysis of Efficacy and Safety. *Vasc Endovascular Surg* **51**, 215-219, doi:10.1177/1538574417698905 (2017).

11 Langhorne, P., Bernhardt, J. & Kwakkel, G. Stroke rehabilitation. *Lancet* **377**, 1693-1702, doi:10.1016/S0140-6736(11)60325-5 (2011).

12 Billinger, S. A. *et al.* Physical activity and exercise recommendations for stroke survivors: a statement for healthcare professionals from the American Heart Association/American Stroke Association. *Stroke* **45**, 2532-2553, doi:10.1161/STR.0000000000000022 (2014).

13 Fleet, A., Page, S. J., MacKay-Lyons, M. & Boe, S. G. Modified constraint-induced movement therapy for upper extremity recovery post stroke: what is the evidence? *Top Stroke Rehabil* **21**, 319-331, doi:10.1310/tsr2104-319 (2014).

14 Willems, D. *et al.* Determining the need for in-patient rehabilitation services post-stroke: results from eight ontario hospitals. *Healthc Policy* **7**, e105-118 (2012).

15 Murphy, T. H. & Corbett, D. Plasticity during stroke recovery: from synapse to behaviour. *Nat Rev Neurosci* **10**, 861-872, doi:10.1038/nrn2735 (2009).

16 Cramer, S. C. Repairing the human brain after stroke: I. Mechanisms of spontaneous recovery. *Ann Neurol* **63**, 272-287, doi:10.1002/ana.21393 (2008).

17 Cook, D. J. *et al.* Hydrogel-delivered brain-derived neurotrophic factor promotes tissue repair and recovery after stroke. *J Cereb Blood Flow Metab* **37**, 1030-1045, doi:10.1177/0271678X16649964 (2017).

18 Belayev, L. *et al.* A novel neurotrophic therapeutic strategy for experimental stroke. *Brain Res* **1280**, 117-123, doi:10.1016/j.brainres.2009.05.030 (2009).

19 Cramer, S. C. Treatments to Promote Neural Repair after Stroke. *J Stroke* **20**, 57-70, doi:10.5853/jos.2017.02796 (2018).

20 Domeniconi, M. & Filbin, M. T. Overcoming inhibitors in myelin to promote axonal regeneration. *J Neurol Sci* **233**, 43-47, doi:10.1016/j.jns.2005.03.023 (2005).
21 Cramer, S. C., Enney, L. A., Russell, C. K., Simeoni, M. & Thompson, T. R. Proof-of-Concept Randomized Trial of the Monoclonal Antibody GSK249320 Versus Placebo in Stroke Patients. *Stroke* **48**, 692-698, doi:10.1161/STROKEAHA.116.014517 (2017).
22 Chollet, F. *et al.* Fluoxetine for motor recovery after acute ischaemic stroke (FLAME): a randomised placebo-controlled trial. *Lancet Neurol* **10**, 123-130, doi:10.1016/S1474-4422(10)70314-8 (2011).
23 Jacobs, B. L. & Fornal, C. A. Serotonin and motor activity. *Curr Opin Neurobiol* **7**, 820-825 (1997).
24 Avram, S., Shaposhnikov, S., Buiu, C. & Mernea, M. Chondroitin sulfate proteoglycans: structure-function relationship with implication in neural development and brain disorders. *Biomed Res Int* **2014**, 642798, doi:10.1155/2014/642798 (2014).
25 Koh, C. H., Pronin, S. & Hughes, M. Chondroitinase ABC for neurological recovery after acute brain injury: systematic review and meta-analyses of preclinical studies. *Brain Inj* **32**, 715-729, doi:10.1080/02699052.2018.1438665 (2018).
26 Burnside, E. R. *et al.* (2018).
27 Brown, C. E., Li, P., Boyd, J. D., Delaney, K. R. & Murphy, T. H. Extensive turnover of dendritic spines and vascular remodeling in cortical tissues recovering from stroke. *J Neurosci* **27**, 4101-4109, doi:10.1523/JNEUROSCI.4295-06.2007 (2007).
28 Takatsuru, Y. *et al.* Neuronal circuit remodeling in the contralateral cortical hemisphere during functional recovery from cerebral infarction. *J Neurosci* **29**, 10081-10086, doi:10.1523/JNEUROSCI.1638-09.2009 (2009).
29 Johansen-Berg, H. *et al.* The role of ipsilateral premotor cortex in hand movement after stroke. *Proc Natl Acad Sci U S A* **99**, 14518-14523, doi:10.1073/pnas.222536799 (2002).
30 Wahl, A. S. *et al.* Neuronal repair. Asynchronous therapy restores motor control by rewiring of the rat corticospinal tract after stroke. *Science* **344**, 1250-1255, doi:10.1126/science.1253050 (2014).
31 Manganotti, P. *et al.* Motor disinhibition in affected and unaffected hemisphere in the early period of recovery after stroke. *Clin Neurophysiol* **113**, 936-943 (2002).
32 Swayne, O. B., Rothwell, J. C., Ward, N. S. & Greenwood, R. J. Stages of motor output reorganization after hemispheric stroke suggested by longitudinal studies of cortical physiology. *Cereb Cortex* **18**, 1909-1922, doi:10.1093/cercor/bhm218 (2008).
33 Clarkson, A. N., Huang, B. S., Macisaac, S. E., Mody, I. & Carmichael, S. T. Reducing excessive GABA-mediated tonic inhibition promotes functional recovery after stroke. *Nature* **468**, 305-309, doi:10.1038/nature09511 (2010).
34 Hiu, T. *et al.* Enhanced phasic GABA inhibition during the repair phase of stroke: a novel therapeutic target. *Brain* **139**, 468-480, doi:10.1093/brain/awv360 (2016).
35 Reinkensmeyer, D. J. *et al.* Computational neurorehabilitation: modeling plasticity and learning to predict recovery. *J Neuroeng Rehabil* **13**, 42, doi:10.1186/s12984-016-0148-3 (2016).
36 Brown, C. E., Aminoltejari, K., Erb, H., Winship, I. R. & Murphy, T. H. In vivo voltage-sensitive dye imaging in adult mice reveals that somatosensory maps lost to stroke are replaced over weeks by new structural and functional circuits with prolonged modes of activation within both the peri-infarct zone and distant sites. *J Neurosci* **29**, 1719-1734, doi:10.1523/JNEUROSCI.4249-08.2009 (2009).
37 Lim, D. H., LeDue, J. M., Mohajerani, M. H. & Murphy, T. H. Optogenetic mapping after stroke reveals network-wide scaling of functional connections and heterogeneous

recovery of the peri-infarct. *J Neurosci* **34**, 16455-16466, doi:10.1523/JNEUROSCI.3384-14.2014 (2014).

38 Silasi, G. & Murphy, T. H. Stroke and the connectome: how connectivity guides therapeutic intervention. *Neuron* **83**, 1354-1368, doi:10.1016/j.neuron.2014.08.052 (2014).

39 Auriat, A. M., Neva, J. L., Peters, S., Ferris, J. K. & Boyd, L. A. A Review of Transcranial Magnetic Stimulation and Multimodal Neuroimaging to Characterize Post-Stroke Neuroplasticity. *Front Neurol* **6**, 226, doi:10.3389/fneur.2015.00226 (2015).

40 Wilson, M. T. & St George, L. Repetitive Transcranial Magnetic Stimulation: A Call for Better Data. *Front Neural Circuits* **10**, 57, doi:10.3389/fncir.2016.00057 (2016).

41 Kang, N., Summers, J. J. & Cauraugh, J. H. Transcranial direct current stimulation facilitates motor learning post-stroke: a systematic review and meta-analysis. *J Neurol Neurosurg Psychiatry* **87**, 345-355, doi:10.1136/jnnp-2015-311242 (2016).

42 Kang, N., Weingart, A. & Cauraugh, J. H. Transcranial direct current stimulation and suppression of contralesional primary motor cortex post-stroke: a systematic review and meta-analysis. *Brain Inj*, 1-8, doi:10.1080/02699052.2018.1481526 (2018).

43 Meyers, E. C. *et al.* Vagus Nerve Stimulation Enhances Stable Plasticity and Generalization of Stroke Recovery. *Stroke* **49**, 710-717, doi:10.1161/STROKEAHA.117.019202 (2018).

44 Hulsey, D. R. *et al.* Reorganization of Motor Cortex by Vagus Nerve Stimulation Requires Cholinergic Innervation. *Brain Stimul* **9**, 174-181, doi:10.1016/j.brs.2015.12.007 (2016).

45 Dawson, J. *et al.* Safety, Feasibility, and Efficacy of Vagus Nerve Stimulation Paired With Upper-Limb Rehabilitation After Ischemic Stroke. *Stroke* **47**, 143-150, doi:10.1161/STROKEAHA.115.010477 (2016).

46 Ward, N. S. Non-invasive brain stimulation for stroke recovery: ready for the big time? *J Neurol Neurosurg Psychiatry* **87**, 343-344, doi:10.1136/jnnp-2015-311991 (2016).

47 Jones, T. A. & Adkins, D. L. Motor System Reorganization After Stroke: Stimulating and Training Toward Perfection. *Physiology (Bethesda)* **30**, 358-370, doi:10.1152/physiol.00014.2015 (2015).

48 Kubis, N. Non-Invasive Brain Stimulation to Enhance Post-Stroke Recovery. *Front Neural Circuits* **10**, 56, doi:10.3389/fncir.2016.00056 (2016).

49 Cheng, M. Y. *et al.* Optogenetic neuronal stimulation promotes functional recovery after stroke. *Proc Natl Acad Sci U S A* **111**, 12913-12918, doi:10.1073/pnas.1404109111 (2014).

50 Shah, A. M. *et al.* Optogenetic neuronal stimulation of the lateral cerebellar nucleus promotes persistent functional recovery after stroke. *Sci Rep* **7**, 46612, doi:10.1038/srep46612 (2017).

51 Buetefisch, C. M. Role of the Contralesional Hemisphere in Post-Stroke Recovery of Upper Extremity Motor Function. *Front Neurol* **6**, 214, doi:10.3389/fneur.2015.00214 (2015).

52 Biernaskie, J., Szymanska, A., Windle, V. & Corbett, D. Bi-hemispheric contribution to functional motor recovery of the affected forelimb following focal ischemic brain injury in rats. *Eur J Neurosci* **21**, 989-999, doi:10.1111/j.1460-9568.2005.03899.x (2005).

53 Dancause, N., Touvykine, B. & Mansoori, B. K. Inhibition of the contralesional hemisphere after stroke: reviewing a few of the building blocks with a focus on animal models. *Prog Brain Res* **218**, 361-387, doi:10.1016/bs.pbr.2015.01.002 (2015).

54 Pernia, M. *et al.* c-Fos and Arc/Arg3.1 expression in auditory and visual cortices after hearing loss: Evidence of sensory crossmodal reorganization in adult rats. *J Comp Neurol* **525**, 2677-2689, doi:10.1002/cne.24233 (2017).
55 Guzowski, J. F., Setlow, B., Wagner, E. K. & McGaugh, J. L. Experience-dependent gene expression in the rat hippocampus after spatial learning: a comparison of the immediate-early genes Arc, c-fos, and zif268. *J Neurosci* **21**, 5089-5098 (2001).
56 Clarke, J., Langdon, K. D. & Corbett, D. Early poststroke experience differentially alters periinfarct layer II and III cortex. *J Cereb Blood Flow Metab* **34**, 630-637, doi:10.1038/jcbfm.2013.237 (2014).
57 Sompuram, S. R., Vani, K., Tracey, B., Kamstock, D. A. & Bogen, S. A. Standardizing Immunohistochemistry: A New Reference Control for Detecting Staining Problems. *J Histochem Cytochem* **63**, 681-690, doi:10.1369/0022155415588109 (2015).
58 Cao, V. Y. *et al.* Motor Learning Consolidates Arc-Expressing Neuronal Ensembles in Secondary Motor Cortex. *Neuron* **86**, 1385-1392, doi:10.1016/j.neuron.2015.05.022 (2015).
59 Broussard, G. J., Liang, R. & Tian, L. Monitoring activity in neural circuits with genetically encoded indicators. *Front Mol Neurosci* **7**, 97, doi:10.3389/fnmol.2014.00097 (2014).
60 DeNardo, L. & Luo, L. Genetic strategies to access activated neurons. *Curr Opin Neurobiol* **45**, 121-129, doi:10.1016/j.conb.2017.05.014 (2017).
61 Zhong, Z. A. *et al.* Optimizing tamoxifen-inducible Cre/loxp system to reduce tamoxifen effect on bone turnover in long bones of young mice. *Bone* **81**, 614-619, doi:10.1016/j.bone.2015.07.034 (2015).
62 Lyford, G. L. *et al.* Arc, a growth factor and activity-regulated gene, encodes a novel cytoskeleton-associated protein that is enriched in neuronal dendrites. *Neuron* **14**, 433-445 (1995).
63 Denny, C. A. *et al.* Hippocampal memory traces are differentially modulated by experience, time, and adult neurogenesis. *Neuron* **83**, 189-201, doi:10.1016/j.neuron.2014.05.018 (2014).
64 Root, C. M., Denny, C. A., Hen, R. & Axel, R. The participation of cortical amygdala in innate, odour-driven behaviour. *Nature* **515**, 269-273, doi:10.1038/nature13897 (2014).
65 Guenthner, C. J., Miyamichi, K., Yang, H. H., Heller, H. C. & Luo, L. Permanent genetic access to transiently active neurons via TRAP: targeted recombination in active populations. *Neuron* **78**, 773-784, doi:10.1016/j.neuron.2013.03.025 (2013).
66 Perusini, J. N. *et al.* Optogenetic stimulation of dentate gyrus engrams restores memory in Alzheimer's disease mice. *Hippocampus* **27**, 1110-1122, doi:10.1002/hipo.22756 (2017).
67 Ye, L. *et al.* Wiring and Molecular Features of Prefrontal Ensembles Representing Distinct Experiences. *Cell* **165**, 1776-1788, doi:10.1016/j.cell.2016.05.010 (2016).
68 Bouet, V. *et al.* The adhesive removal test: a sensitive method to assess sensorimotor deficits in mice. *Nat Protoc* **4**, 1560-1564, doi:10.1038/nprot.2009.125 (2009).
69 Shiotsuki, H. *et al.* A rotarod test for evaluation of motor skill learning. *J Neurosci Methods* **189**, 180-185, doi:10.1016/j.jneumeth.2010.03.026 (2010).
70 Ren, M., Cao, V., Ye, Y., Manji, H. K. & Wang, K. H. Arc regulates experience-dependent persistent firing patterns in frontal cortex. *J Neurosci* **34**, 6583-6595, doi:10.1523/JNEUROSCI.0167-14.2014 (2014).
71 Clarkson, A. N. *et al.* AMPA receptor-induced local brain-derived neurotrophic factor signaling mediates motor recovery after stroke. *J Neurosci* **31**, 3766-3775, doi:10.1523/JNEUROSCI.5780-10.2011 (2011).

72 Ceizar, M., Hasu, M., Lagace, DC. Increasing progenitor cell survival is insufficient to improve stroke recovery. Department of Cellular and Molecular Medicine, University of Ottawa, Ontario, Canada. Poster presented at the 6th Annual Canadian Stroke Congress. September 2015.
73 Muñoz, W., Tremblay, R., Levenstein, D. & Rudy, B. Layer-specific modulation of neocortical dendritic inhibition during active wakefulness. *Science* **355**, 954-959, doi:10.1126/science.aag2599 (2017).
74 Ye, L. *et al.* TRPV4 is a regulator of adipose oxidative metabolism, inflammation, and energy homeostasis. *Cell* **151**, 96-110, doi:10.1016/j.cell.2012.08.034 (2012).
75 Ashley, J. *et al.* Retrovirus-like Gag Protein Arc1 Binds RNA and Traffics across Synaptic Boutons. *Cell* **172**, 262-274.e211, doi:10.1016/j.cell.2017.12.022 (2018).
76 Pastuzyn, E. D. *et al.* The Neuronal Gene Arc Encodes a Repurposed Retrotransposon Gag Protein that Mediates Intercellular RNA Transfer. *Cell* **172**, 275-288.e218, doi:10.1016/j.cell.2017.12.024 (2018).
77 Peters, A. J., Liu, H. & Komiyama, T. Learning in the Rodent Motor Cortex. *Annu Rev Neurosci* **40**, 77-97, doi:10.1146/annurev-neuro-072116-031407 (2017).
78 Weiler, N., Wood, L., Yu, J., Solla, S. A. & Shepherd, G. M. Top-down laminar organization of the excitatory network in motor cortex. *Nat Neurosci* **11**, 360-366, doi:10.1038/nn2049 (2008).
79 Volz, L. J. *et al.* Time-dependent functional role of the contralesional motor cortex after stroke. *Neuroimage Clin* **16**, 165-174, doi:10.1016/j.nicl.2017.07.024 (2017).
80 Dodd, K. C., Nair, V. A. & Prabhakaran, V. Role of the Contralesional vs. Ipsilesional Hemisphere in Stroke Recovery. *Front Hum Neurosci* **11**, 469, doi:10.3389/fnhum.2017.00469 (2017).
81 Bastani, A. & Jaberzadeh, S. Does anodal transcranial direct current stimulation enhance excitability of the motor cortex and motor function in healthy individuals and subjects with stroke: a systematic review and meta-analysis. *Clin Neurophysiol* **123**, 644-657, doi:10.1016/j.clinph.2011.08.029 (2012).
82 Rehme, A. K., Eickhoff, S. B., Rottschy, C., Fink, G. R. & Grefkes, C. Activation likelihood estimation meta-analysis of motor-related neural activity after stroke. *Neuroimage* **59**, 2771-2782, doi:10.1016/j.neuroimage.2011.10.023 (2012).
83 Murase, N., Duque, J., Mazzocchio, R. & Cohen, L. G. Influence of interhemispheric interactions on motor function in chronic stroke. *Ann Neurol* **55**, 400-409, doi:10.1002/ana.10848 (2004).